Master of Science thesis in meteorology

CASE STUDY OF A EUROPEAN MEDIUM-RANGE WEATHER FORECAST BUST

Lauri Tuppi

11.8.2017

Supervisor(s): Victoria Sinclair PhD

Examiners: Victoria Sinclair PhD and prof. Heikki Järvinen

UNIVERSITY OF HELSINKI
DEPARTMENT OF PHYSICS

POB 64 (Gustaf Hällströmin katu 2)
00014 University of Helsinki

HELSINGIN YLIOPISTO – HELSINGFORS UNIVERSITET – UNIVERSITY OF HELSINKI

Tiedekunta/Osasto – Fakultet/Sektion – Faculty/Section	Laitos – Institution – Department	
Tekijä – Författare – Author		
Työn nimi – Arbetets titel – Title		
Oppiaine – Läroämne – Subject		
Työn laji – Arbetets art – Level	Aika – Datum – Month and year	Sivumäärä – Sidoantal – Number of pages
Tiivistelmä – Referat – Abstract		
Avainsanat – Nyckelord – Keywords		
Säilytyspaikka – Förvaringställe – Where deposited		
Muita tietoja – Övriga uppgifter – Additional information		

HELSINGIN YLIOPISTO – HELSINGFORS UNIVERSITET – UNIVERSITY OF HELSINKI

Tiedekunta/Osasto – Fakultet/Sektion – Faculty/Section	Laitos – Institution – Department	
Tekijä – Författare – Author		
Työn nimi – Arbetets titel – Title		
Oppiaine – Läroämne – Subject		
Työn laji – Arbetets art – Level	Aika – Datum – Month and year	Sivumäärä – Sidoantal – Number of pages
Tiivistelmä – Referat – Abstract		
Avainsanat – Nyckelord – Keywords		
Säilytyspaikka – Förvaringställe – Where deposited		
Muita tietoja – Övriga uppgifter – Additional information		

Contents

1. Introduction

The modern world is used to accurate and reliable weather forecasts. Many make their plans even a week ahead based on weather forecasts. People rely much on weather forecasts. Usually the weather will be what had been predicted but this is not always the case. Occasionally numerical weather prediction (NWP) models encounter a weather pattern that is not easily forecastable and then the forecasts may fail. These cases of sudden poor predictive skill of the forecasts are always totally or almost totally unexpected. Sometimes it can, though, be possible to guess that something might be about to happen. Ensemble forecasts or groups of slightly different forecasts may show increased spread preceding a bad forecast so that the ensembles offer multiple different possible weather scenarios. It is still impossible to know which one of the scenarios is about to become reality.

It is not surprising that people become upset when the forecast they relied so much on fails miserably. Another aspect is that the failed forecasts cause extra expenses. One may take expensive precautions for bad weather but the forecast bad weather never came or another way around one may not prepare for bad weather based on the forecast and the weather causes damage. These cases always cause a storm of angry feedback from the public and also the author of this thesis has got a part of it. This is the motivation to study one case of such failed forecast. Before the forecasts can be improved we have to know in details what happens in the forecast when it fails and where is the reason for the failure.

For this study I chose a case of badly performing six days long medium range forecast initiated on the 10th of April 2011 at 00 UTC. Hereafter a bad forecast is called a forecast bust. This case is a typical spring time forecast bust that is related to North American convection. However, in general there are also other sources of forecast busts besides convection but this study does not address these other sources.

Previous studies e.g. Rodwell et al. (2013) and Grazzini and Isaksen (2002) have already investigated European forecast busts. Grazzini and Isaksen (2002) conducted a case by case study of European forecast busts and concluded that the busts have something to do with convective activity over the Great Lakes´ area in the United States. Rodwell et al. (2013) brought a large scale point of view and linked the busts and convective activity over the United States to Rossby wave dynamics. In this study I will reproduce some results shown in those two studies but I will also go

deeper in details. I will look both at the evolution of convection over the US and evolution of large scale Rossby wave dynamics after the convective event. I will also try to find initial conditions which produce a better forecast using ensemble forecast.

The purpose of this study is to determine if the incorrect representation of convection over North America lead to a forecast bust over Europe. First I take a look how do the control forecast and ensemble members differ from reanalysis on the 6th day of the forecast over Europe and second, I consider early stage errors in precipitation CAPE and Rossby wave source fields over the US. The effects of upper level divergence caused by convection on large scale dynamics are considered with Rossby wave source and potential vorticity. Third, I try to find forecast skill improving patterns from initial conditions of an ensemble forecast of 10 April 2011 00 UTC.

2. Background

2.1. Forecast busts

A forecast bust means a situation when a NWP model predicted a very different weather pattern than what eventually came true. In the most extreme cases, NWP models can, for example, forecast rainy weather related to a trough, but instead a ridge arrives bringing sunny weather or other way around. NWP models occasionally have difficulties to capture transitions from one weather regime to another (Reinhold 1987). A “weather regime” can be defined as a quasi stable flow configuration (Reinhold 1987). One frequently occurring and well known flow configuration is the Scandinavian Blocking where a high pressure system sits over Scandinavia for several days, and upper level geopotential height contours above resemble Greek letter Ω.

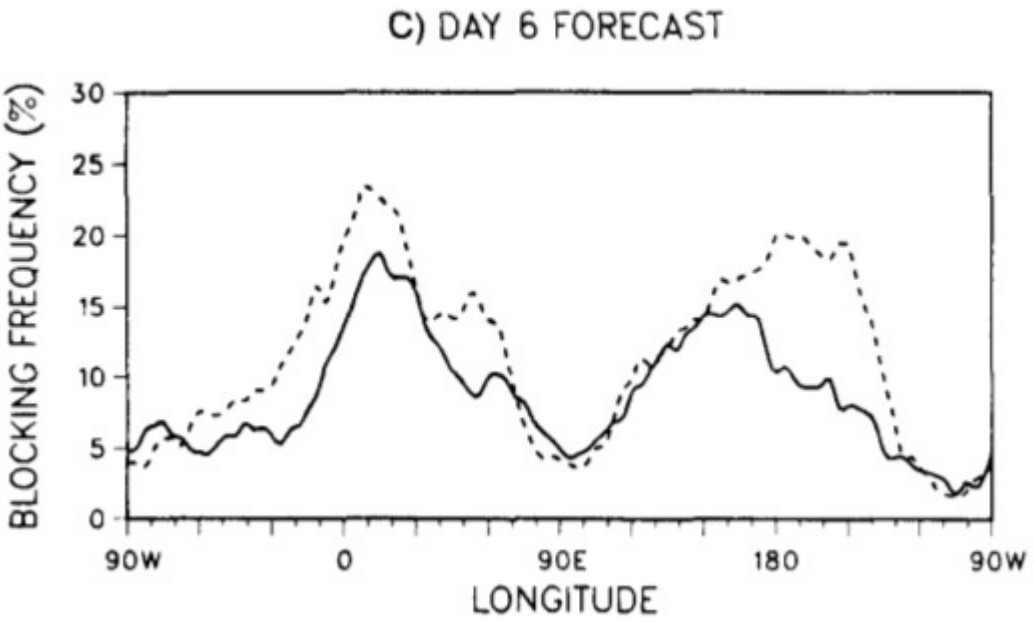

Figure 1. Observed blocking frequency (dashed line) and average modelled blocking frequency (solid line) according to general circulation model of ECMWF on latitude 60° N. Here blocking is defined so that typically southward pointing 500 hPa geopotential height gradient is very small or even reversed (Tibaldi and Molteni 1990).

Tibaldi and Molteni (1990) studied forecasts from seven winter periods from 1980-81 to 1986-87. They state that already in 6 day forecasts, models tend to create a climate of their own. NWP models typically under-represent blocking configurations, and especially they seem to have difficulties in entering to the blocked regime, and they tend to conserve westerly flow instead. At least more than 25 year old NWP models seem to have such a property that the modelled climate does not represent the actual climate in longer iterations. Usually the flow becomes too zonal, and there are too few blocking situations, and they often occur in untypical places (figure 1). This is already seen in 6 day forecast but the underestimation and shift of the maxima of blocking become even more pronounced in longer iterations (Tibaldi and Molteni 1990). This problem has become smaller in modern models, but it has not vanished entirely (Tibaldi and Molteni 1990).

Once the models have entered into blocking regime, they occasionally have troubles with breakdowns of these regimes so that they underestimate the persistence of the blocking regimes. Models may predict that the breakdown occurs several days too early. Reinhold (1987) has traced the causes of sudden breakdowns of blocking

to extreme weather events. Rodwell et al. (2013) also suggest that this April 2011 forecast bust case discussed later in details in this study is related to misrepresented blocking event over Europe.

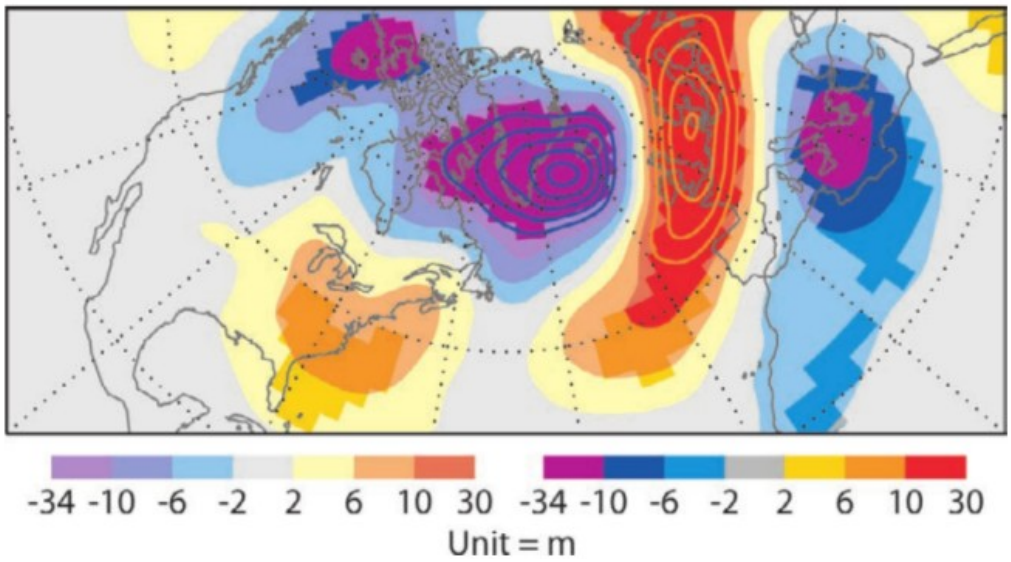

Figure 2. Verifying analysis anomaly of 500 hPa geopotential height from ERA-Interim reanalysis climatology for 584 bust cases in 1989 – 2008. Verifying analysis is used to monitor skill of operational forecasts. It is relative to reanalysis but here it can be considered as the truth so the figure represents the average of departures of true weather patterns from climatology during the forecast busts so that positive (negative) values mean that the 500 hPa geopotential height was higher (lower) in the verifying analyses than in the climatology during the busts. Bold colours indicate level of 5% statistical significance using the t-test. Dipole pattern of high pressure over North-western Europe and low pressure over the Mediterranean point to production of cut-off lows due to the anticyclonic Rossby wave breaking. (Rodwell et al. 2013).

Rodwell et al. (2013) created a composite of European forecast busts using cycle 31r2 of Integrated Forecasting System (IFS) which is used in ERA-Interim reanalysis system (Dee et al. 2011). That version of OpenIFS was operational from December 2006 to June 2007. Rodwell et al. (2013) compared the day 6 forecast verifying analyses to ERA-Interim climatology. Figure 2 suggests that there is statistically significant high pressure over North-western Europe during the busts on average so the forecasts missed the development of high pressures. There is also a low pressure in the Mediterranean, which suggests that the busts are related to anticyclonic Rossby wave breaking (Rodwell et al. 2013). More information about the Rossby wave breaking is in chapter 2.4.

If the NWP models and initial conditions were perfect, then all forecasts would

be perfect. Of course, the models and initial conditions contain some imperfections. The sensitivity of NWP models to errors in initial conditions varies significantly, and also the degree of initial errors varies. In these paragraphs model sensitivity should not be confused with model error. Model sensitivity means sensitivity to initial conditions and parameter uncertainty, and model error means error in representation of physics in a model. Here I am discussing about the model sensitivity. Sometimes the NWP models can be so sensitive that even a very small difference in initial conditions or in parametrisations can lead to very different results. On the other hand, situations where there is extreme convection, are prone for generation of large errors in initial conditions. One obvious reason for this is that data assimilation is occasionally struggling to combine observations and modelled data (Grazzini and Isaksen 2002).

Modern data assimilation is done by minimizing the cost function in four dimensions i.e. the task is to find a state which is between the modelled state and the observed state and is as close to both as possible in three space and one time dimension. This 4D variational data assimilation is computationally heavy and time consuming procedure so the minimization of the cost function is usually stopped after only a couple of iterations. When there is, for example, strong convection occurring in a different location than predicted, the difference between the modelled field and the “true” field may not decrease enough during only a couple of iterations so the cost function is nowhere near the minimum. The analysis increment is the difference between the first guess forecast and the final analysis (Grazzini and Isaksen 2002), and it is an indicator of possible errors in initial conditions produced by data assimilation. If the analysis increments were large, the possibility of errors in initial conditions is also large. One area of frequent large analysis increments is the central United States where there usually occur numerous strong meso-scale convective systems (MCS) in spring and early summer (Grazzini and Isaksen 2002).

Although errors in initial conditions are large factors in failed forecasts, usually they cannot cause a forecast bust only by themselves, but also some kind of dynamic

Figure 3. Illustration of behaviour of the Lorenz 63 modelwith two different regimes. The panels show how dynamic instability depends on the initial state. Yellow dots are possible states of the model, black circles and dots represent ensemble forecasts with slightly different initial states. In panel (a), the model is stable, and all the slightly perturbed forecasts remain close to each other, and deviation is small. In panel (b), the instability of the model has increased. Now transition from one regime to another becomes possible. Panel (c) represents a case when the instability of the model is very large as small differences in initial conditions leads to large deviation. (Kalnay 2010). A real world example of unstable model is in figure 4.

instability of NWP model is needed. Let dynamic instability mean that even a small perturbation in initial conditions can cause the model to end up in very different state. One moment when the effect of dynamic instability can sometimes be seen is transition from one weather regime to another. A simplified example of dynamic

instability can be presented using Lorenz 63 model (L63), (Lorenz 1963). L63 is a chaotically behaving non-linear model which still stays in control in rather a small domain. L63 has two separated regimes (figure 3).

When the model is stable, all of the model runs initiated with slightly different initial states end up quite close to each other so there is not much spread, and predictability is good (panel a). On the other hand, when the model is unstable, the runs may even end up in different regimes (panel c). The spread among the perturbed runs is also very large now and predictability is poor. This example was extremely simple but the same principle applies also to more complex models. NWP models can have multiple regimes to explore, but in Europe the two dominant regimes are westerly flow and blocking. Figure 4 shows how the dynamic instability can be seen in real forecasts. For the first few days the spread among the ensemble members is rather small and the model is dynamically stable (compare to panel (a) in figure 3) but the spread starts to increase on the 8th of April (compare to panel (b) in figure 3) and peaks on the 10th when some members are in blocked regime, some are in regime of westerly flow and some are somewhere in between (compare to panel (c) in figure 3). Contradictory to panel (c) in figure 3, the ensemble members do not spread equally in two regimes in figure 4. On the 10th of April only 7 of 51 ECMWF forecasts entered into the correct regime or exceeded the 40% mark of anomaly correlation coefficient (ACC) that is the treshold of forecast bust.

Rodwell et al. (2013) defined a forecast bust to be an event when the ACC of 500 hPa geopotential height over Europe drops below 40% on the sixth day of the forecast. The ACC is a skill score, and a skill score is a measure that can be used to measure how good a forecast is. The ACC can be calculated using formula (Inness and Dorling 2013)

$$ACC = \frac{\sum (F-C)(A-C)}{\sqrt{\sum (F-C)^2 (A-C)^2}} \quad (1)$$

where F is forecast value, A is value from reanalysis or analysis or it is some other value representing the “truth”, and C is the climatology. The range goes from -100% to 100% and 100% means that the forecast is perfect. 50% means that the forecast is not better than climatology used as forecast and -100% means that the forecast is “a mirror image” of the analysis so that there are troughs in the forecast where there are ridges in the analysis and vice versa. Typically the ACC of a 6 day forecast is between 75% and 90% and it is exceptional that it drops below 40%. That is why

Rodwell et al. (2013) defined a forecast bust to be a case when the ACC of 6 day forecast drops below 40%. The ACC takes into account both the deviation of the forecast from the climatology, and the deviation of the reanalysis from the climatology. Therefore the ACC weighs more anomalous weather patterns which deviate significantly from climatology for example blocking high pressure systems. The ACC is usually computed over some limited area in the grid. The ACC quantifies the similarity of the forecast pattern to reanalyzed pattern i.e. do the plotted maps look similar or not. The ACC can be used only for continuous scalar fields, for example, geopotential height or temperature. It cannot be used to discontinuous fields, like precipitation, because of the "double penalty" of location errors. Double penalty means that, for example, precipitation occurring in different location than predicted decreases the ACC two times more than an occasion when the area of precipitation is completely missing. The double penalty causes so much white noise that any signal is impossible to distinguish.

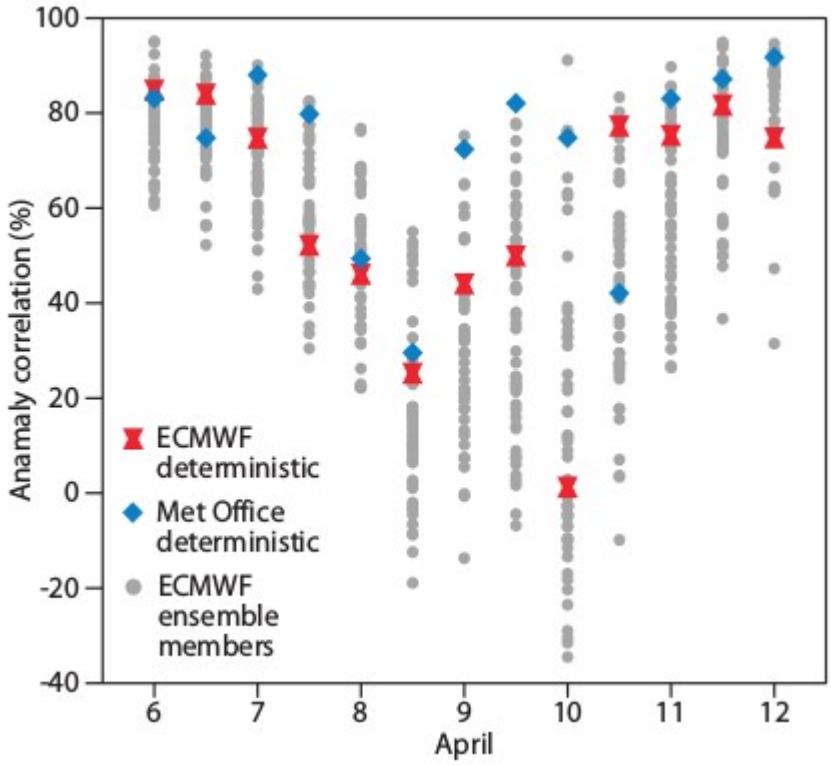

Figure 4. The anomaly correlation coefficient as a function of the initialisation date of day 6 forecasts. Coloured polygons represent deterministic forecasts of ECMWF and the UK Met Office. Grey dots represent the 50 ensemble members of the ensemble forecasts of ECMWF. (Rodwell et al. 2013). Although this is related to the April 2011 bust case, this figure also serves as general example of performance of ensemble forecast during a forecast bust.

Figure 5 shows the time evolution of the forecast bust selected for this study. One can see that this is not a troublesome time to initiate forecast only for ECMWF but several major numerical weather prediction centers around the world also suffered of this forecast bust. There are differences in how quickly the skill of the forecasts of different models recovered. Although I chose a forecast bust that occurred over Europe, Rodwell et al. (2013) remind that forecast busts are not a problem only in Europe but they occur also elsewhere in the world.

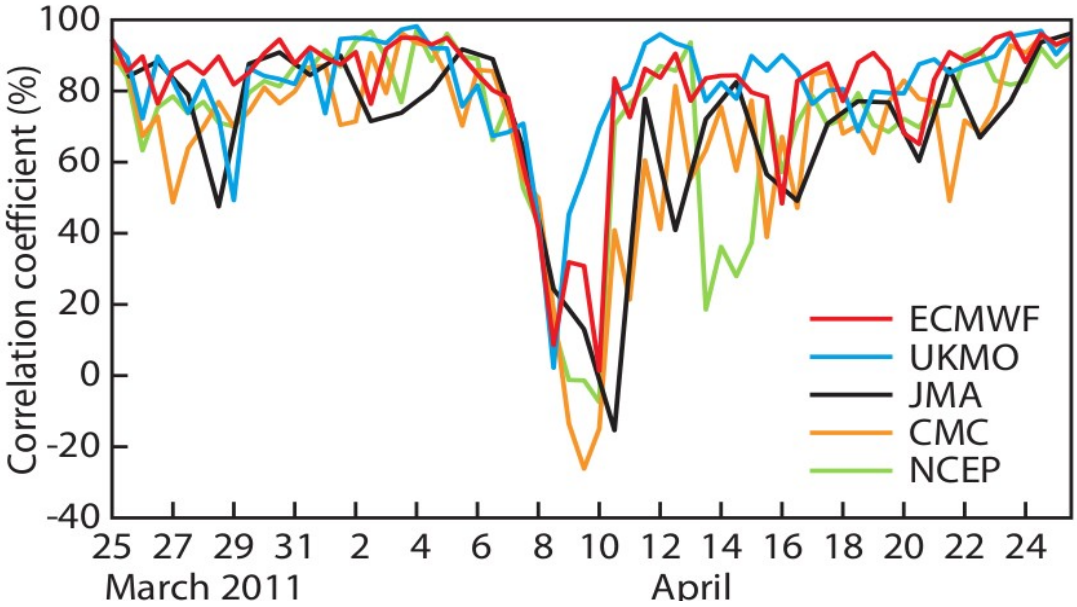

Figure 5. Time series of anomaly correlation coefficient (ACC) of day 6 forecasts over Europe calculated from forecasts produced by some of the world´s numerical weather prediction centers: European Centre for Medium-Range weather Forecasts (ECMWF), the UK Met Office (UKMO), Japan Meteorological Agency (JMA), Canadian Meteorological Centre (CMC) and National Centre for Environmental Prediction (NCEP). On the x-axis the dates are the initialisation dates of the 6 day forecasts. ACC is a measure of how good the forecast is. Before the 7th and after the 11th of April 2011 most of the forecasts perform well but between the 7th and 11th all of the forecasts presented in the figure encounter problems (Rodwell et al. 2013).

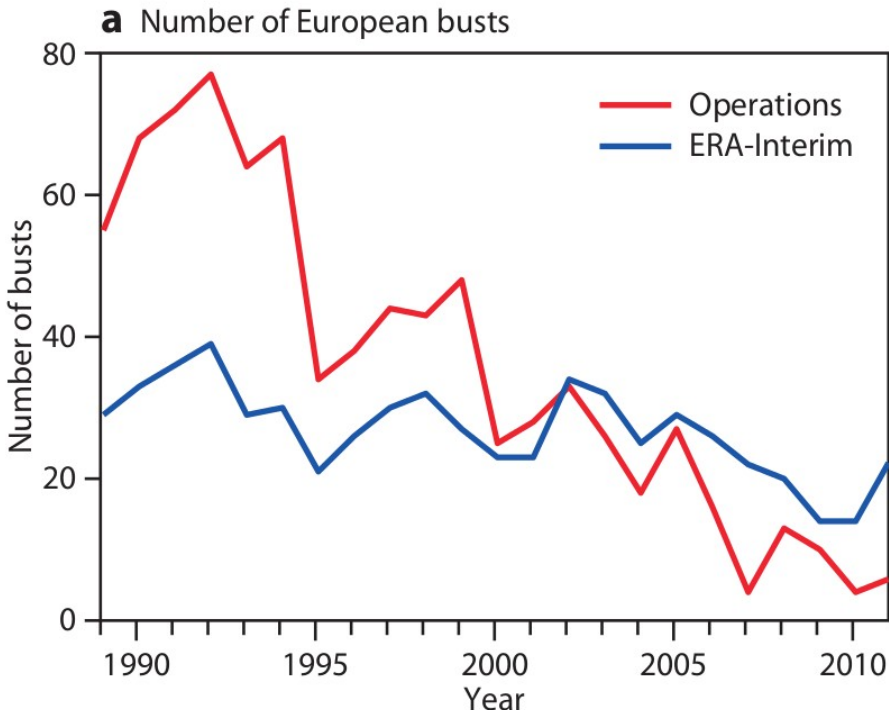

Figure 6. Annual totals of European forecast busts of 6 day forecasts in IFS and ERA-Interim of ECMWF. The number of busts has been decreasing fast with developing model and better initial conditions. ERA-Interim instead uses fixed model version so the number has not decreased so fast (Rodwell et al. 2013).

The number of forecast busts has decreased significantly during past years (figure 6) and most of the busts are not so severe any more. Usually the ACC drops only slightly below 40%. Nowadays there occur only a couple of busts a year in Integrated Forecast System (IFS) which is the operational forecasting system at ECMWF, and not all of them are as severe as the April 2011 bust discussed in this study. Figure 6 shows the development of ECMWF forecasts. Improvements have taken place as initial conditions have become better, model parametrisations has been developed and resolution has been increased as computational resources have increased. Now then model resolutions have been multiplied, more and more small scale phenomena can be calculated explicitly and this reduces the need of parametrizations which have caused model error before. One way to improve weather forecasts is to improve accuracy of the initial conditions as number of iterations of the cost function in data assimilation can be increased as computational resources increase. Many of large forecast errors have been traced to initial conditions but improving initial conditions is not fast and easy either. The quality of initial conditions is on one hand limited by computational resources and 4D

variational assimilation is difficult to make more efficient and on the other hand strongly determined by the number and quality of the actual observations. Another rather inexpensive but not very practical method in operational usage is to enhance initial conditions of the previous day by deducing optimal perturbations from one day forecast and reanalysis and then run a longer forecast with enhanced initial conditions (Pu et al. 1997).

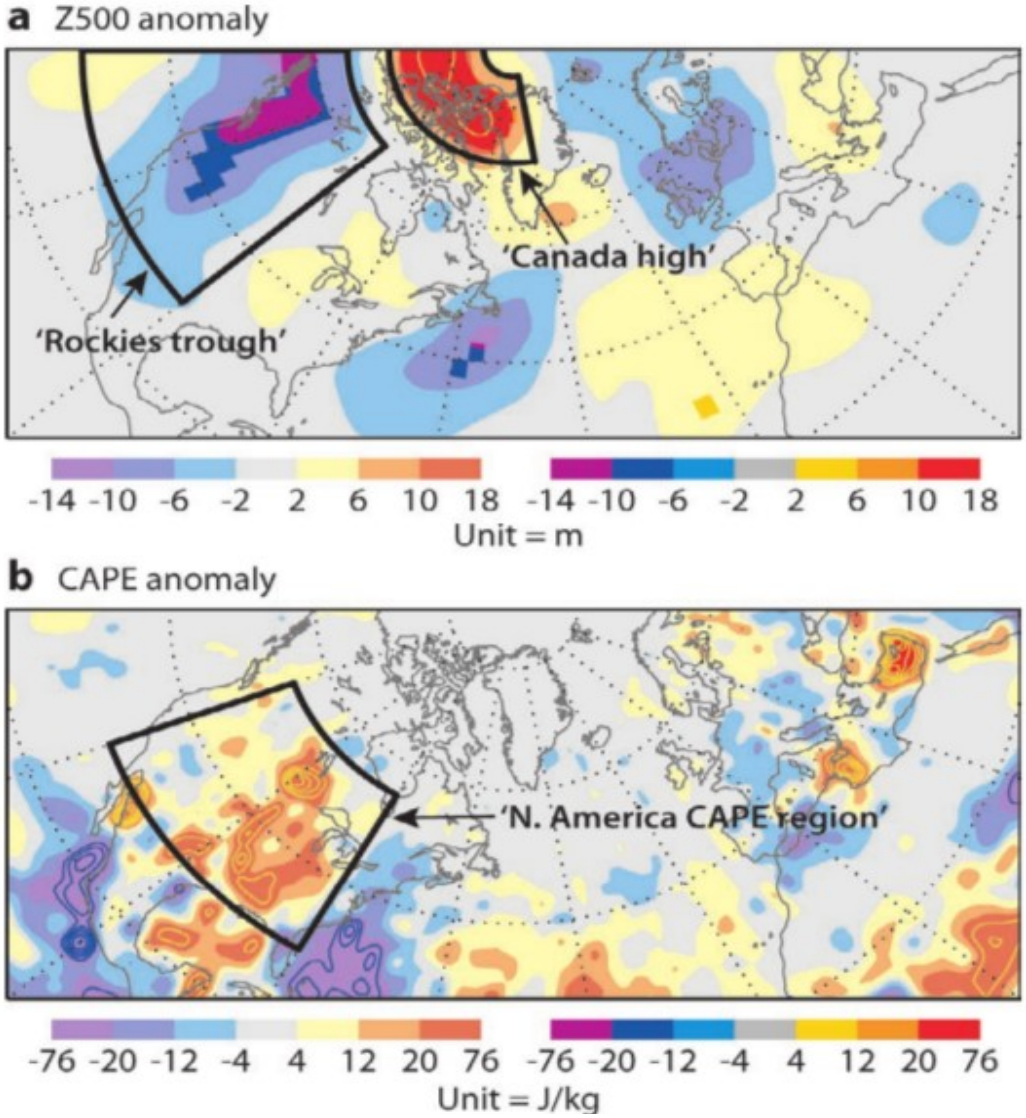

Figure 7. Mean initial condition anomalies of a) 500 hPa geopotential height and b) CAPE leading to forecast busts in 6 day forecasts. There are in total 584 forecast busts from the 1st of January 1989 to the 24th of June 2010. Anomalies are relative to ERA-Interim climatology for 1989 to 2008. Bold colours indicate statistical significance at 5% level using the t-test. (Rodwell et al. 2013).

Rodwell et al. (2013) have also studied what are the typical atmospheric

conditions over North America before a European forecast bust using forecasts generated with ERA-Interim. They discovered that before a bust, there are areas of higher than usual convective available potential energy (CAPE) (figure 7b) and a weak ridge in American Mid-West, and a trough over the Rockies (figure 7a). There is also the statistically significant Canada high in figure 7a but Rodwell et al. (2013) suggest that it does not affect the forecast busts significantly. The trough-ridge pattern and areas of high CAPE are present also in the 10 April 2011 forecast bust case as will be seen in chapter 4.1.

2.2. Introduction to vorticity and potential vorticity

Vorticity and potential vorticity (PV) are crucial terms when investigating atmospheric flow structures. Vorticity and PV play key roles in the dynamics of the Rossby waves which determine the weather regime. Rossby waves are large scale atmospheric waves caused by varying planetary vorticity. More information about Rossby waves is in chapters 2.3., 2.4. and 2.5. Vorticity represents shear or curvature of the flow. Absolute vorticity consists of two parts: relative vorticity and planetary vorticity. Relative vorticity means the shear and curvature of flow respect to the ground and planetary vorticity comes from the rotation of the Earth. Meteorologists often consider only the vertical part of the vorticity

$$\eta = \boldsymbol{k}.\nabla \times \boldsymbol{v} + f \qquad (2)$$

where η is absolute vorticity, **v** is the horizontal 2D wind vector respect to the ground, f is planetary vorticity and **k** is the unit vector aligned along vertical z-axis. Only vertical component is often considered as vertical wind velocity is much smaller than horizontal velocity.

Vorticity can be changed via divergence and convergence and changing vorticity changes the Rossby waves. The vorticity equation (Holton and Hakim 2011 p. 107)

$$\left(\frac{\partial}{\partial t} + \boldsymbol{v}.\nabla\right)\eta = \eta\frac{\partial \omega}{\partial p} + \boldsymbol{k}.(\nabla \times \boldsymbol{F}) \qquad (3)$$

describes the connection between vorticity and divergence. In the equation [3] **v** is horizontal wind vector, η is absolute vorticity, ω is vertical motion in pressure coordinates and **F** is friction vector. In the free atmosphere the last friction term can be neglected and because of the law of continuity

$$\frac{\partial \omega}{\partial p} = \nabla . \boldsymbol{v} \quad , \tag{4}$$

the differential vertical velocity can be replaced with divergence to obtain vorticity equation in the free atmosphere

$$(\frac{\partial}{\partial t} + \boldsymbol{v} . \nabla)\eta = \eta(\nabla . \boldsymbol{v}) \quad . \tag{5}$$

The vorticity equation basically tells that divergence decreases and convergence increases absolute vorticity. This is an analogue to the conservation of angular momentum. For example if a rotating skater moves arms and legs closer to the body, angular velocity must increase and vice versa.

PV is by definition absolute circulation that is enclosed between two isentropic surfaces (Holton and Hakim 2011 p. 112). Potential vorticity equation is

$$PV = \frac{\zeta_\theta + f}{\rho}\frac{\partial \theta}{\partial z} = -g(\zeta_\theta + f)\frac{\partial \theta}{\partial p} \tag{6}$$

where I have changed the coordinate system using the hydrostatic balance. In the equation ρ is density of air, g is the gravity constant, ζ_θ is relative vorticity on an isentropic surface, and θ is potential temperature. In practice surfaces of constant potential temperature are almost always almost horizontal so as a first assumption I can replace ζ_θ with the vertical component of relative vorticity ζ. As can be seen from the formula, PV is product of absolute vorticity and static stability. PV is also conserved for adiabatic, frictionless geostrophic motion (Lackmann 2011 p. 89). Therefore one can identify the origins of air masses in the upper troposphere and in stratosphere where there are quite little diabatic processes and friction. On isentropic surfaces the PV tends to increase from south to north so it is easy to see polar air surging equatorward and vice versa. This is very useful quality of PV when detecting Rossby wave breaking. Conservation of PV has also other consequences. When air masses are advecting meridionally, vorticity and stability terms of PV must balance each other. If an air parcel is moving north (south), vorticity is increasing (decreasing) so stability must decrease (increase). Poleward advecting tropical air mass has to become less statically stable as planetary vorticity increases. The unit of PV is impractical $m^{-2}\ s^{-1}\ K\ kg^{-1}$, so it is more convenient to introduce the potential vorticity unit PVU. The value of one PVU is $10^{-6}\ m^{-2}\ s^{-1}\ K\ kg^{-1}$. Tropospheric PV values are from 0 to 2 PVUs. Often the value of 2 PVUs is defined to be the dynamic tropopause. In stratosphere the PV values are high due to strong static stability.

2.3. Rossby waves

Ascent caused by mountains, largescale forcing or convection cause upper level wind to diverge and due to conservation of circulation in the vorticity equation horizontal flow gains anticyclonic relative vorticity and turns towards equator. When this air mass has advected to lower latitudes, its absolute vorticity has become larger than local planetary vorticity so the air mass has gained now cyclonic relative vorticity and turns back towards higher latitudes. Then the oscillation begins again. This horizontal oscillation is called the Rossby wave. Rossby waves exist because the Coriolis parameter and planetary vorticity vary respect to latitude (Holton and Hakim 2011 p. 160).

There are two types of Rossby waves. Ones are stationary and usually caused by mountain ranges. Whereas others are transient and caused by for example heating and convection. These transient Rossby waves are the ones who partly determine the transitions between weather regimes over Europe. Evolution of these transient Rossby waves preceding the forecast bust will be examined in this study. Propagation speed of the Rossby waves depends on horizontal wind speed and wave length. Phase speed of an individual Rossby wave is always westward relative to the mean zonal flow. The phase speed is (Holton and Hakim 2011 p. 162)

$$c=\frac{\nu}{k}=\frac{uk}{k}-\frac{1}{k}\frac{df}{dy}\frac{k}{k^2+l^2}=u-\frac{\beta}{k^2+l^2} \tag{7}$$

where ν is frequency, u is zonal mean wind, f is the planetary vorticity, k and l are zonal and meridional wave numbers and β is the meridional derivative of planetary vorticity. The group velocity of Rossby waves is (Holton and Hakim 2011 p. 162)

$$c_g=\frac{\partial \nu}{\partial k}=u+\beta\frac{k^2-l^2}{(k^2+l^2)^2} \quad . \tag{8}$$

As the group velocity is larger than the phase speed, Rossby wave groups propagate faster than individual waves. It can be shown also that energy is moving at group velocity: new waves forming in front of the old ones get the energy from old waves. Therefore it is more likely that wave groups transport errors from North America to Europe than individual waves. Even though Rossby wave groups propagate significantly faster eastward than individual waves, they do not arrive to Europe in an instant. For example one can assume zonal wind of 30 ms^{-1}, latitude of 45ºN, zonal wave length of 6000 km, no meridional waves and distance from American

Mid West to Central Europe to be 8000 km. Then one can use equation [8] and obtain that it would take over three days for the Rossby wave group to arrive in Central Europe. That is why errors originating from North America cannot be seen in short (< 3 days) forecasts.

Rossby waves cannot be seen in everyday surface weather charts because friction damps very efficiently wavy movement close to the ground. To some extent Rossby wave can be observed in 500 hPa or in higher level geopotential height charts. On those levels geopotential height contours form wavy patterns but as geopotential height typically increases towards equator because of warming air, it is often difficult to distinguish where the Rossby wave begins and where it ends. The figures can be made significantly clearer by subtracting zonal mean from geopotential height field. Then one can see zonal and meridional structure of the Rossby waves more clearly. Another means to detect Rossby waves is to look at the PV charts. Especially the boundary of tropical and polar air masses can be seen very clearly. The wavy nature of this boundary is due to the Rossby waves. The boundary also tells about other qualities of the Rossby waves like how they break. The Rossby wave breaking will be considered in further details in chapter 2.5.

Average amplitude of the Rossby waves varies during the course of a year so that the waves are the most amplified in winter and spring and the least amplified in summer (Ahlquist 1985).

2.4. The Rossby wave source

One might think that what part of the vorticity equation [5] corresponds to the advection and what part to the amplification or destruction of the Rossby waves. The terms cannot be seen straightly from the vorticity equation as terms on the both sides contain partly both advection and forcing. The advection and forcing terms can be separated by doing some manipulations to the vorticity equation according to James (1994 p. 263 - 268). First I split the horizontal wind vector **v** into rotational and divergent components

$$\boldsymbol{v} = \boldsymbol{v}_\psi + \boldsymbol{v}_\chi \qquad (9)$$

where the rotational wind vector $\mathbf{v}_\psi$ is given by

$$\boldsymbol{v}_\psi = \boldsymbol{k} \times \nabla \psi \quad ; \qquad (10)$$

the cross product of unit vector **k** and the gradient of the stream function ψ. The divergent wind vector $\mathbf{v}_\chi$ is given by

$$\boldsymbol{v}_\chi = \nabla \chi \quad ; \tag{11}$$

the gradient of the velocity potential χ. Next I substitute **v** with $\mathbf{v}_\psi$ and $\mathbf{v}_\chi$ and rearrange the vorticity equation to obtain

$$\left(\frac{\partial}{\partial t} + \boldsymbol{v}_\psi . \nabla\right)\eta = -\boldsymbol{v}_\chi . \nabla \eta - D\eta \quad , \tag{12}$$

where η is the absolute vorticity and D is divergence of the wind. In this form the left hand side represents the advection and the right hand side the forcing of the Rossby waves.

The forcing term

$$S = -\boldsymbol{v}_\chi . \nabla \eta - D\eta \tag{13}$$

is called the Rossby wave source (RWS). Thus, this form is qualitatively difficult to understand. It is difficult to see which one of the terms dominates. The first term on the right hand side of equation [13] is often small but not necessarily. To combine the terms I transform equation [13] to qualitatively more easily understandable form using vector identities (not shown)

$$S = -\nabla . (\boldsymbol{v}_\chi \eta) \quad . \tag{14}$$

The typical order of magnitude of the RWS obtained from scale analysis is 10^{-8} s^{-2}. Positive and negative values can mean both generation and destruction of Rossby waves depending on the location. Positive (negative) values in a ridge and negative (positive) values in a trough lead to amplification (destruction) of the Rossby waves. Equation [14] shows that amplification of Rossby waves is strong in strong gradient of divergent wind in area of nonzero absolute vorticity i.e. outside of the equatorial region. Typical areas of large RWS locate in subtropics because tropical convection causes upper level divergence at the equator and strong divergent wind which points towards areas of descent in subtropics. Then this strong divergent wind is affected by increasing absolute vorticity due to increasing coriolis force at higher latitudes. Also convection occurring elsewhere than in the tropics causes upper level divergent wind so it is meaningful to consider RWS in the case of North American convection.

2.5. Rossby wave breaking

Occasionally strong RWS can transform initially zonal flow to mode with very high amplitude Rossby waves. These amplified waves are prone to break. Rossby wave breaking (RWB) can be defined so that PV contours are “overturned” (Thorncroft et al. 1993). This means that PV values decrease significantly northwards on constant potential temperature surface as PV usually decreases southwards. Another definition is that PV gradient of perturbation exceeds that of zonal mean. Usually RWB can be seen on the maps as encircled or almost encircled areas of high or low PV or alternatively high or low dynamic tropopause. In fact RWB can be detected in a thick layer between upper troposphere and lower mesosphere (Hitchman and Huesmann 2007) but I limit this study to the surroundings of the tropopause. RWB leads to irreversible mixing of air masses. A characteristic of RWB is the production of streamers and cut-off lows where there are areas of encircled high PV. RWB is also suggested to be related with onset of anomalous quasi persistent weather regimes like blocking high pressures (Postel and Hitchman 1999).

There are four ways how Rossby waves can break: warm anticyclonic, cold anticyclonic, warm cyclonic and cold cyclonic (Masato et al. 2011). Whether the wave breaking is warm or cold is determined by relative sizes of forming warm and cold anomalies. In warm (cold) wave breaking, the warm (cold) anomaly is larger than the cold (warm) anomaly. For simplicity I do not consider relative sizes of the anomalies but I limit to only consider cyclonic and anticyclonic wave breaking.

One way of breaking is breaking anticyclonically equatorward called life cycle one (LC1) and the other way is breaking cyclonically poleward called life cycle two (LC2) (Thorncroft et al. 1993). LC1 is characterized by relatively weak Norwegian type of cyclones and strong anticyclones (Thorncroft et al. 1993). When Rossby wave is breaking anticyclonically, the part of the wave closest to the equator usually hardly moves zonally. Instead it can be moving meridionally towards equator (figure 8 a). The part closer to the pole continues moving eastward and eventually whole wave falls frontward and connection of the equatorward pushing trough to polar air breaks. Anticyclonic wave breaking resembles a cross section of shallow water wave breaking on shore. Anticyclonic wave breaking has been linked to diffluent jet (Schultz et al. 1998) so it is most likely to occur over oceans and west coasts of continents so it is relatively common over North Atlantic and Europe.

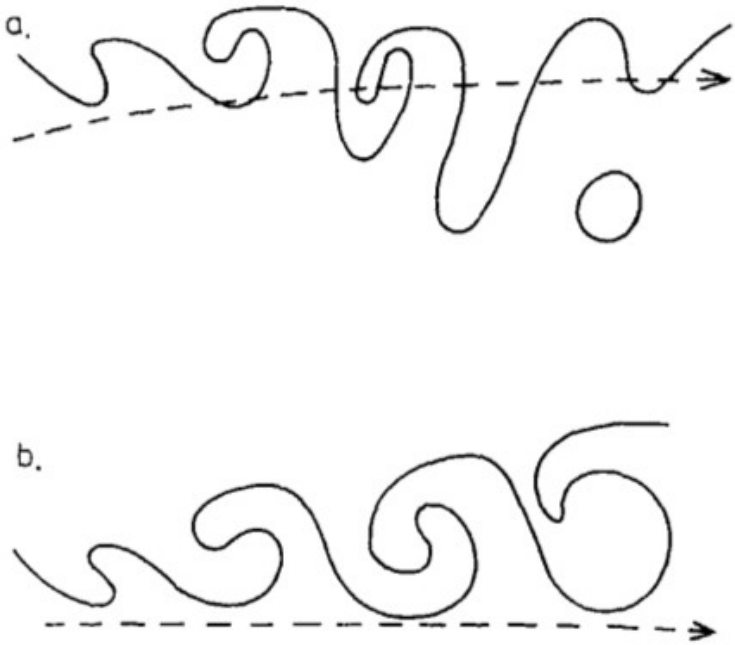

Figure 8. The life cycles of PV contours on constant potential temperature (solid curves) and approximate positions of jet axes (dashed lines). Panel (a) represents the anticyclonic way of breaking (LC1) where the Rossby wave becomes meridionally very elongated and breaks to the direction of propagation (right). Panel (b) represents the cyclonic way of breaking (LC2) where the low PV air from lower latitudes wraps around the centre of a strong trough. Both LC1 and LC2 tend to produce cut-off lows eventually (Thorncroft et al. 1993).

LC2 is related to strong Shapiro-Keyser type cyclones and weak ridges (Schultz et al. 1998). When Rossby wave breaks cyclonically, the low PV air in front of the low pressure wraps around the low centre and meets again the original low PV air behind the low pressure (figure 8 b). The Rossby wave seems to fall backwards. Cyclonic wave breaking has been linked to confluent jet (Schultz et al. 1998) so it is most likely to occur over east coasts of continents. Figure 9 provides a real life example of both anticyclonic and cyclonic wave breaking. Anticyclonic RWB is marked with green ellipse. Warm air originating from tropics has moved north-east and locates north of cooler air from midlatitudes. There is also cyclonic RWB in the red ellipse. Tropical warm air has moved north-west while cold polar air has moved east. Both RWBs have caused almost isolated warm and cold anomalies.

RWB is fairly common phenomenon thorough a year in mid and high latitudes on both hemispheres but it is more common on northern hemisphere (Hitchman and Huesmann 2007) and the RWB activity peaks in summer (Postel and Hitchman

1999).

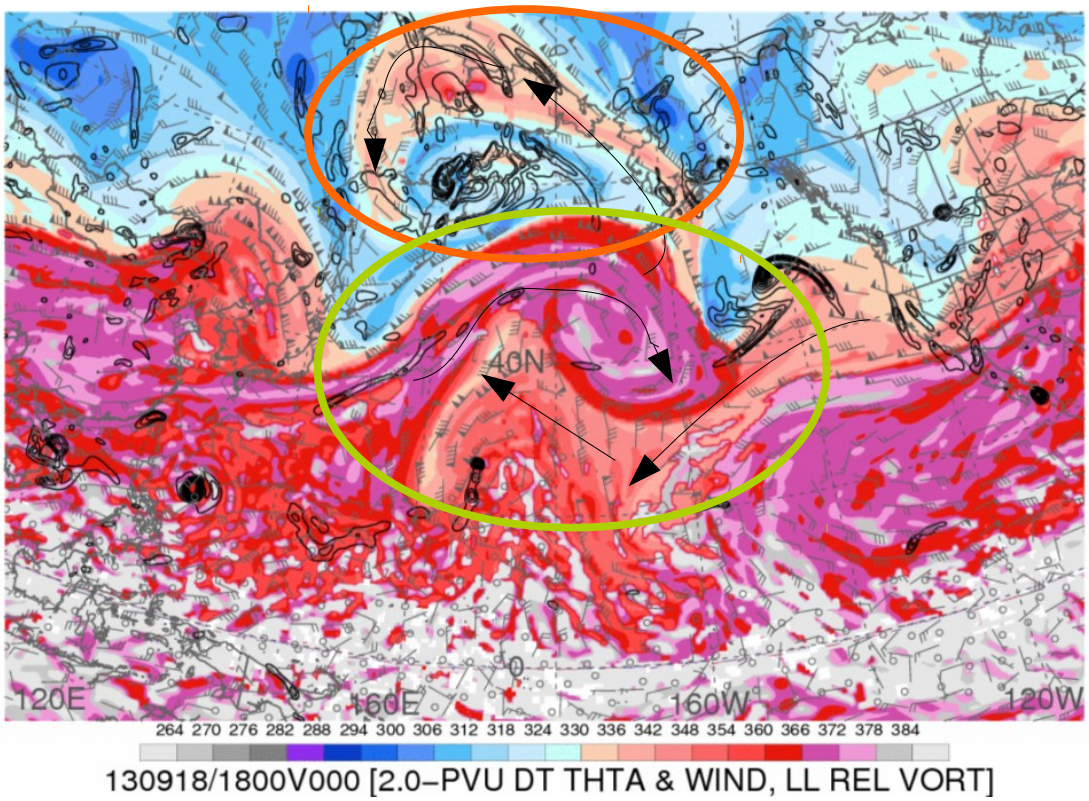

Figure 9. There is an example of both equatorward anticyclonic and poleward cyclonic wave breaking over the Pacific. 2.0 PVU level potential temperature is shaded, 2.0 PVU level wind is denoted with barbs and low level relative vorticity is contoured. The orange ellipse shows cyclonic RWB where warm air wraps cyclonically around cold air. The green ellipse shows anticyclonic RWB where warm air wraps anticyclonically around cold air. Both wave breakings have produced almost isolated areas that are considerably warmer than the surroundings. (GFS Analysis 2014)

2.6. Quasi geostrophic terminology

There will be a statement in the results section that trough axis is leaning westwards with height and therefore the surface low is intensifying. What does this mean? The intensification can be explained with the quasi geostrophic omega, height tendency and vorticity equations. The way the equations work will be discussed only qualitatively in this section. When the trough axis is leaning westwards, the surface low is east of the upper level trough. Straight above the surface low there is cyclonic vorticity advection increasing with height as the upper level trough is still approaching from west (figure 10) and cyclonic vorticity advection is small near the

surface. The omega equation states that upwards strengthening cyclonic vorticity advection causes forcing for ascent. Due to the continuity the ascent causes horizontal convergence below. According to the quasi geostrophic vorticity equation convergence leads to increasing cyclonic vorticity and this means that the geopotential height decreases and the surface low intensifies (Ruosteenoja and Räisänen 2013 p. 21).

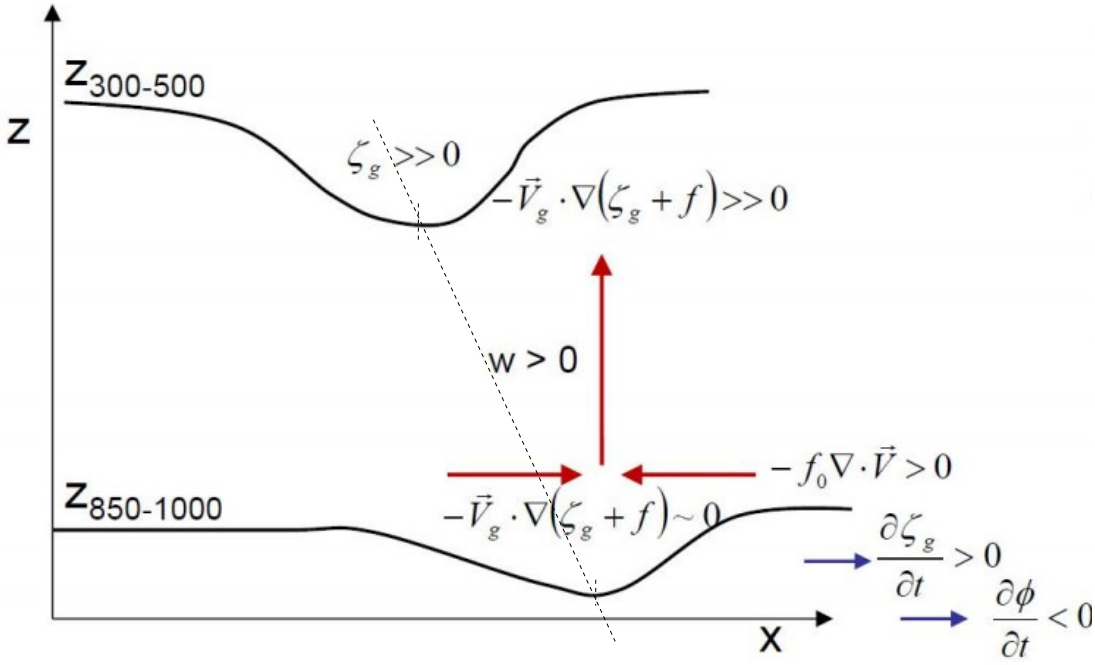

Figure 10. Conceptual model of eastward propagating upper level trough which is intensifying the lower level trough ahead. In the figure ζ_g is the geostrophic relative vorticity, f is the planetary vorticity, $\mathbf{V}_g$ is the geostrophic wind and Φ is the geopotential. In the figure the trough is moving east (right). Above the low level trough there is strong cyclonic vorticity advection which according to the omega equation causes ascent. The ascending air is replaced by converging air in lower levels. According to the quasi geostrophic vorticity equation convergence increases cyclonic vorticity in the low level trough and according to the height tendency equation, incresing cyclonic vorticity decreases geopotential height. (Ruosteenoja and Räisänen 2013, p. 21)

2.7. Ensemble forecasting

An ensemble forecast is a probabilistic forecast. It can be used to reveal other possible outcomes of a forecast besides the control forecast and to tell the

predictability of weather. The spread of an ensemble forecast tells how uncertain a forecast is. For example figure 4 in chapter 2.1. shows that IFS was extremely uncertain of the outcome of the forecast starting on the 10th of April as the spread is large. Ensemble forecasts usually contain several individual forecasts. For example the ensemble of ECMWF contains one deterministic high resolution forecast and 50 ensemble members with lower resolution. The deterministic forecast or control forecast has the best available initial conditions whereas the initial conditions of the ensemble members have been perturbed i.e. there have been added and subtracted some small errors representing possible observation errors. Ensemble forecast is a useful tool in forecasting the predictability. Ensembles are needed as modern NWP models contain parametrizations that may not always be completely realistic. Many small scale phenomena cannot be calculated explicitly. Moreover, many physical processes are not completely understood and they are parametrized based on the best guess of the experts (Ollinaho et al. 2013). Therefore some parametrizations are not the best possible in physical mind and they may cause errors to forecasts. On the other hand it is well known fact that initial conditions are never perfect. There are always errors originating from observations, data assimilation and simplified model parametrizations. The purpose of ensemble is to generate a range of possible outcomes so that the effect of the errors would be represented.

There are actually two ways to create an ensemble forecast. One and probably more familiar way to reader is to use a set of perturbed initial conditions but an ensemble forecast can be created also by using stochastic physics. Stochastic physics means modifying the calculation of tendencies of model physics. The tendencies produced by parametrizations can be manipulated for example with random numbers between 0.99 and 1.01. The background of stochastic physics lies in the fact that the tendencies are not only calculated explicitly but they contain contribution from parametrizations and parametrizations do include small errors.

Stochastic physics generates the model part of the spread of ensemble forecast (Palmer et al. 2009) whereas perturbed initial conditions generate the spread related to errors in observation and data assimilation. ECMWF applies both stochastic physics and perturbed initial conditions at the same time in operational weather forecasting. As I already had evidence (Grazzini and Isaksen 2002) that this forecast bust is primarily caused by errors in initial conditions, I came to a conclusion that ensemble members generated with stochastic physics could have ended up in very

similar outcomes and small spread. I wanted to create substantial spread so I decided to use perturbed initial conditions. The spread increasing effect of stochastic physics could have been relatively small if the influence of errors in initial conditions had been relatively large.

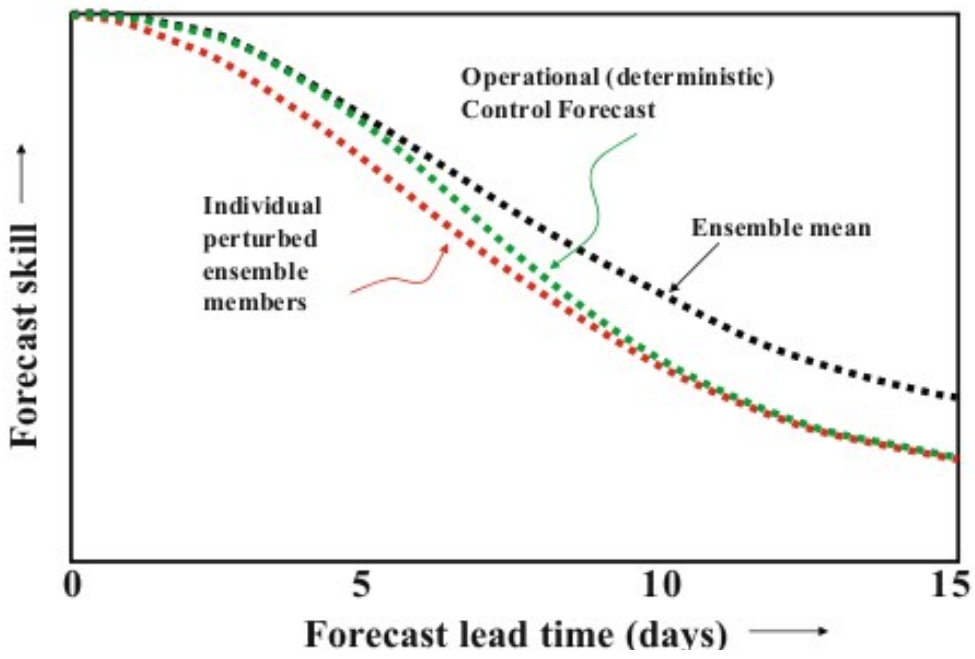

Figure 11. Forecast skill of NCEP GFS forecasts averaged over winter 1997/1998. Skill of the individual perturbed ensemble members (red), operational control forecast (green) and ensemble mean (black) (Lackmann 2011 p. 291, figure 10-43).

Usually forecast skill of the ensemble mean exceeds that of individual perturbed ensemble members and deterministic control forecast (figure 11). This is because the large errors in individual ensemble members largely cancel each other. The better performance of the control forecast in the early part of the forecast is caused by finer resolution (Lackmann 2011 p. 294 – 295). In long run the ACC of the ensemble mean should relax towards 50% because eventually the errors in individual members cancel each other so well that the result begins to resemble the climatology. Indeed, if climatology was used as forecast the ACC would be roughly 50%. Instead the ACC of individual members and the control forecast should fall below 50%. I could say that this example of an average ensemble forecast is a good ensemble forecast. However, when atmosphere transits from one regime to another, the behaviour of ensemble forecast may not be so good anymore.

3. Methods

3.1. OpenIFS and ERA-Interim

In this study I use the Open Integrated Forecasting System (OpenIFS) cycle 38r1 NWP model. IFS cycle 38r1 was the operational model at the ECMWF from the 19th of June 2012 to the 25th of June 2013. OpenIFS is a NWP model without data assimilation so it requires externally generated initial conditions. OpenIFS cannot be used in real-time forecasting. OpenIFS is a spectral, semi-lagrangian global model widely used in research and teaching in the member states of ECMWF (OpenIFS webpages). Resolution of the model in my experiments is spherical truncation T255 with 91 vertical levels, which corresponds to approximately 80 km horizontal grid spacing. I had initial conditions also for higher resolutions T511 and T1279, but I decided to use T255 because the coarse resolution consumed considerably less computational resources, and the post processing and analysis of the output data was fast.

Data from ECMWF Interim Reanalysis (ERA-Interim) (Dee et al. 2011) was used to compare the results produced by OpenIFS. ERA-Interim is based on fixed IFS cycle 31r2 and it contains 4D variational data assimilation system with a 12 hour analysis window. ERA-Interim is based on fixed cycle because change in the forecasts caused by evolution of model has been wanted to be eliminated. Continuously improving operational analyses instead may suffer from inconsistencies related to model development. I could have used operational analyses instead of ERA-Interim in this study, but ERA-Interim data is freely available and easy to download. The resolution of ERA-Interim is T255 with 60 vertical levels the uppermost level being at 0.1 hPa. Temporal resolution is 6 hours but some data is available in 3 hours steps. This is because every other step is actually a 3 hour forecast generated with the model of ERA-Interim. Currently ERA-Interim contains data beginning from the first of January 1979 to almost present day and new data is added in a couple of months delay. In this study ERA-Interim represents the truth although it is possible that the reanalysis data also contains some errors, however, the errors are assumed to be small.

3.2. Experiments conducted

Initially, 13 deterministic forecasts were run with OpenIFS beginning on the 1st and ending on the 13th of April 2011. Every forecast was initialised at 00 UTC. I wanted to verify that the forecast bust also occurs in low resolution OpenIFS for sure as Rodwell et al. (2013) had used operational T1279 high resolution forecasts in their study, and I used lower resolution. After verifying that the bust occurs also in OpenIFS, I took the worst forecast in terms of the ACC initialised on the 10th of April under more precise scrutiny. Hereafter this forecast initialized at 00 UTC 10 April 2011 will be called the control forecast. The aim was to shed light on the errors that caused this forecast to fail. To see how much errors in the initial conditions affect the results, I ran five ensemble members all initialised on the 10th of April.

Besides studying the effect of errors in initial conditions, I tested the effect of changing closure parameters in OpenIFS. Therefore, I ran an experiment with halved entrainment rate of deep convection in which I halved the amount of non-saturated air mixing in convection. However, this method of generating spread proved to be too inefficient. The outcome over Europe did not change much so I abandoned the idea.

To identify the errors and the evolution which lead to the forecast bust over Europe, I analyze the results using the theoretical concepts described in the Background section. I used the ACC to verify the bust and discovered that the entrainment rate experiment was not useful. I also used the ACC to quantify the differences between the ensemble members. The Rossby wave source was used to point out the effect of erroneous divergence over North America caused by misrepresented convection. The PV plots on 315 Kelvin potential temperature surface were used to identify the Rossby wave breaking over the Atlantic. Besides these diagnostics I looked also at the errors in convective available potential energy (CAPE) fields, and 3 and 24 hour total precipitation fields over North America. The errors were calculated by subtracting the ERA-Interim reanalysis field from the forecast field. Over Europe I plotted spaghetti plots of 500 hPa geopotential height from the control forecast and the five ensemble members. The spaghetti plot reveals what really went wrong in the control forecast and are some ensemble members better or not.

As the last task I conducted some further research on the initial conditions of the

ensemble members. I subtracted the initial condition files of the control forecast from the initial condition files of the ensemble members. Then I compared the subtracted files to the ACC of each ensemble member and tried to find patterns which lead to better outcome over Europe 6 days later.

4. Results

4.1. Synoptic scale evolution before and during the convective event

Before the inspection of the errors in convection over North America and consequences over Europe, it is beneficial to understand the synoptic scale configuration over North America before and during the outbreak of strong convection. There are several factors contributing to the formation of two meso-scale convective systems (MCS) over the Central and Eastern United States. Suitable air masses for strong convection were present, and upper level trough and surface low were at the right place at the right time. One strong MCS forms over Nebraska and travels to the Great Lakes and the other one, much weaker MCS, was located in North and South Carolina. The 500 hPa geopotential height maps plotted from ERA-Interim reanalysis data show a deep trough approaching the Mid-West from the Rocky mountains (figure 12). The trough is a lifting trough so it is weakening. Yet it fuels development of surface low pressure system ahead of the trough because the “trough axis” is tilting backwards. The development of the low is not explosive which is also an asset for organised convection (figure 12). The convection was located in close proximity to a warm front so it possibly provided additional forcing. Ahead of the surface low, where the western MCS forms, wind is strongly veering with height due to strong warm advection in Mid-West. This provides wind shear which assists individual storms to cluster into a MCS. This MCS initiates in the blue circle in figure 12. In North and South Carolina there is only speed shear but obviously it was enough to cluster the the storms into MCS also in there.

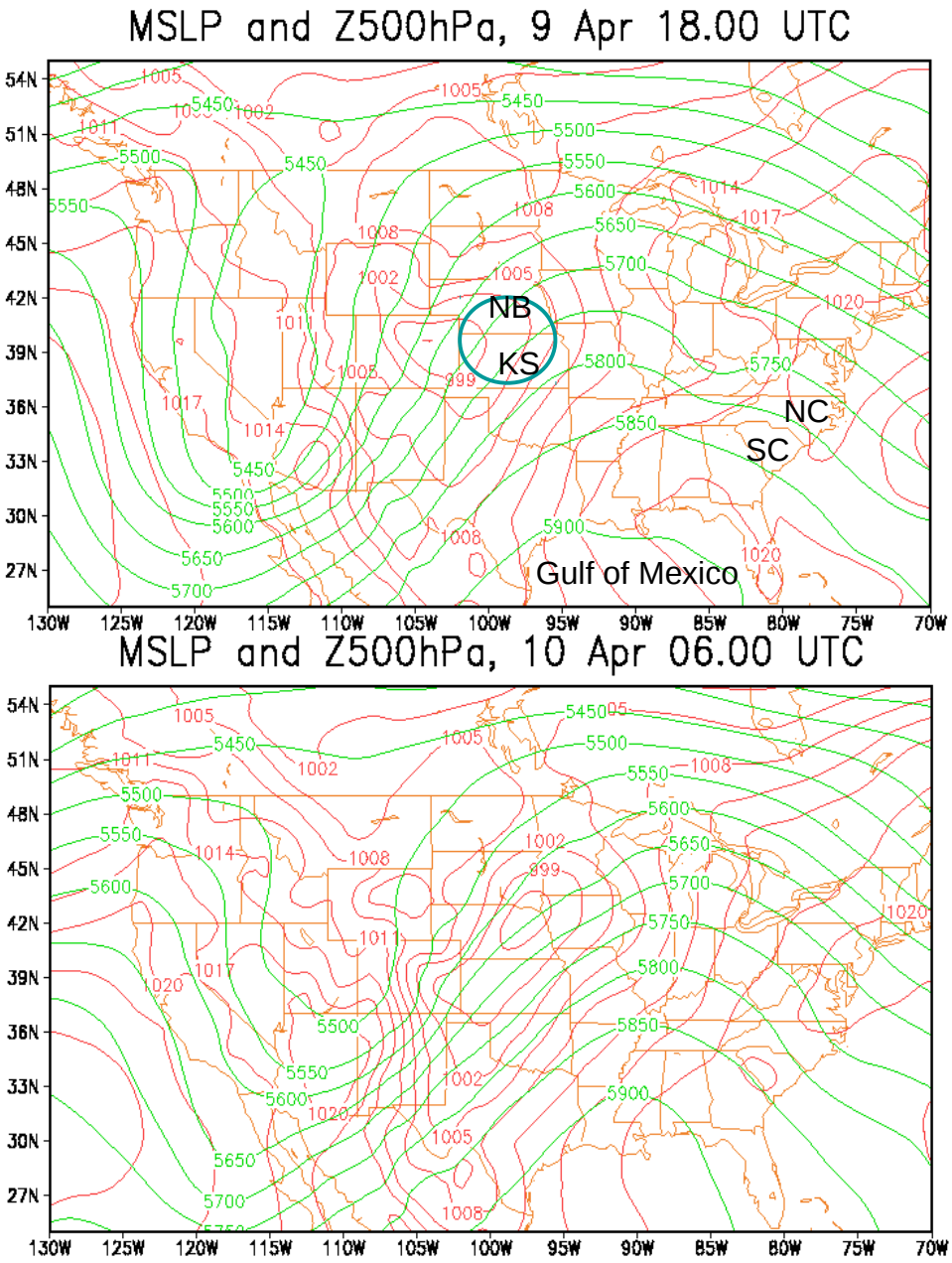

Figure 12. Maps of 500 hPa geopotential height (green contours) and mean sea level pressure (red contours). The upper part is just before the initiation of the MCS in Mid-West at 13.00 local time and the lower part is during the Mid-Western MCS at 01.00 local time. The upper level trough is forcing the surface low to develop slowly although the trough itself is weakening. There is abundant wind shear on the path of the Mid-Western MCS all the way from Southern Nebraska to Northern Wisconsin and Michigan. The wind shear is due to veering wind caused by strong warm advection.

The trough-ridge pattern and high CAPE are observed over the US. This is consistent with the mean initial conditions (figure 7) leading to European forecast bust presented by Rodwell et al. (2013).

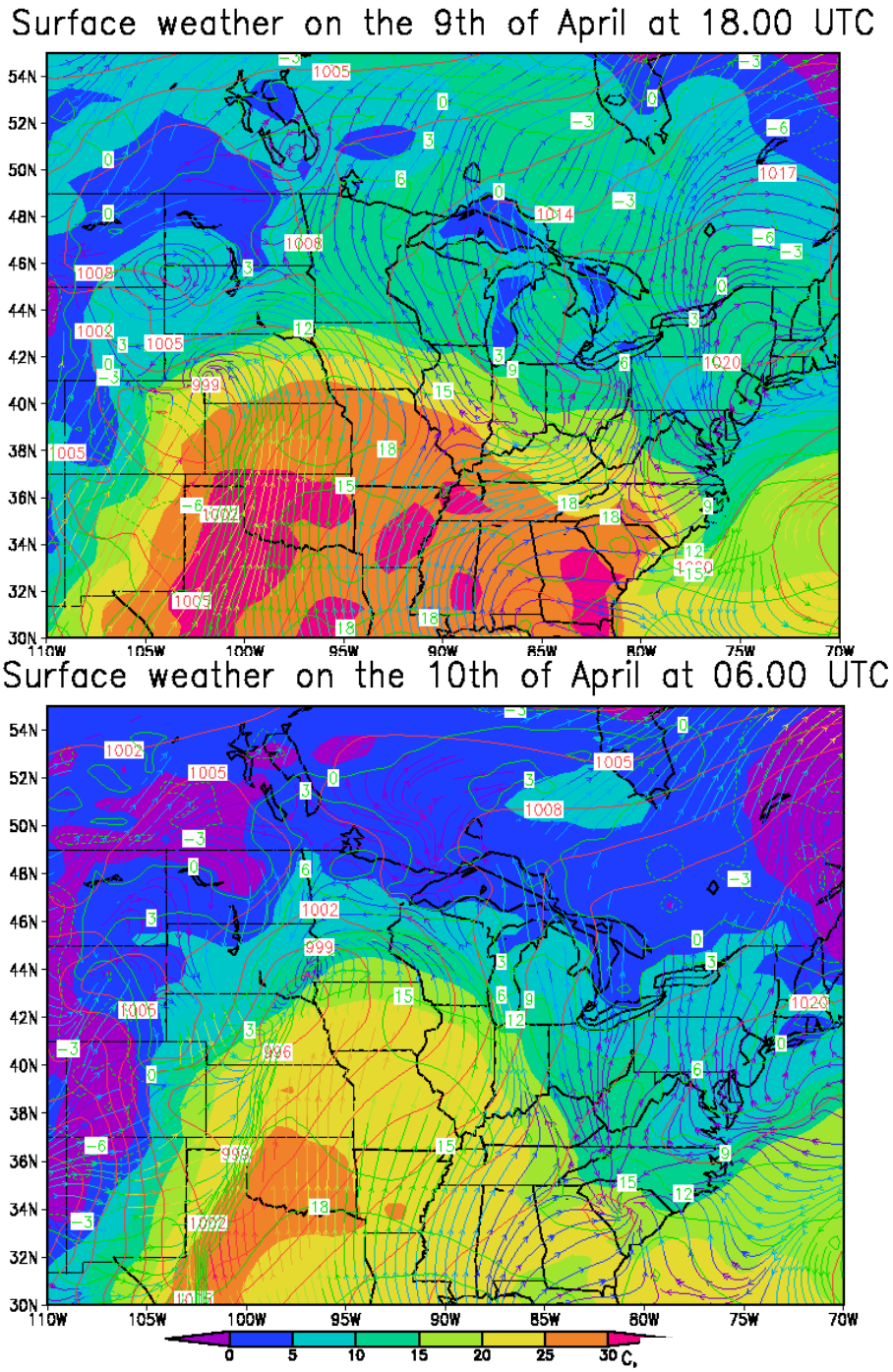

Figure 13. Maps of 2 metre temperature (shaded), 2 metre dew point temperature (green contours), mean sea level pressure (red contours) and 10 metre wind (streamlines). The times are the same as in previous figure. Tropical hot and humid air mass is advecting north in the warm sector of the surface low. The northernmost part of the tropical surface airmass is advecting underneath northward cooling mid and upper tropospheric air. (Compare to figure 12). The advection leads to increasing hydrostatic instability and build-up of CAPE.

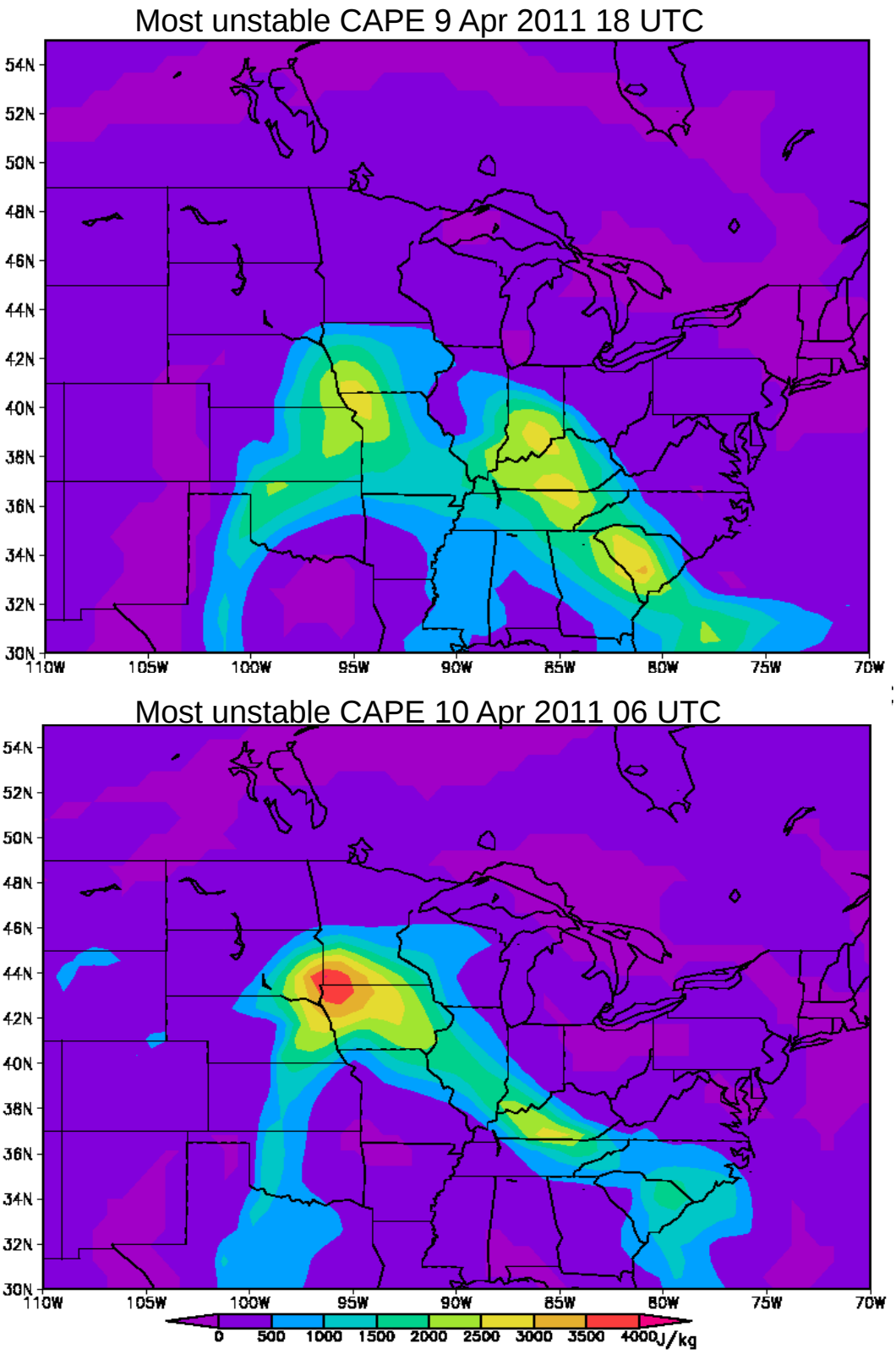

Figure 14. Most unstable CAPE (shaded) before (the upper panel) and after (the lower panel) the initiation of the Mid-Western MCS. Most unstable means that the parcel ascent begins from hydrostatically the most unstable air layer. Advection of tropical air underneath cool air lead to large values of CAPE.

The surface weather maps plotted from ERA-Interim reanalysis data show strong very moist and warm southerly flow straight from Gulf of Mexico on the eastern flank of the surface low (figure 13). In the warm sector of the surface low, 2 metre temperature is around 30 ºC during local day at 18 UTC and 2 metre dew point temperature exceeds locally 18 ºC. Moist air close to the ground generates CAPE. Also the moist air close to the surface is moving underneath northward cooling mid and upper tropospheric air shown by figure 12. This increases the CAPE even more especially in the very northernmost tip of the hot and humid air mass (figure 14). The CAPE peaks around 06.00 UTC on the 10th of April. The peak value of 4000 J/kg west of the Great Lakes is very large. CAPE value of 3000 J/kg in South Carolina is also impressive. All in all conditions for formation of MCS were very favourable in the area west of the Great Lakes and moderately favourable in North and South Carolina.

4.2. Control forecast

The first task to do with the control forecast of the 10th of April and 12 other deterministic forecasts was to check that the bust really occurs also in OpenIFS so it is not only some other malfunction of some part in full IFS itself. I found that the bust also occurs in OpenIFS so the errors lie in the initial conditions constructed from operational analyses or in model parametrisations. I also wanted to find the worst day to start a forecast in OpenIFS. The worst day to start a forecast is the 10th of April like it is also in IFS. IFS, though, produces a double bust on the 8th and the 10th of April (figure 1) whereas OpenIFS produces only a single bust on the 10th (figure 16).

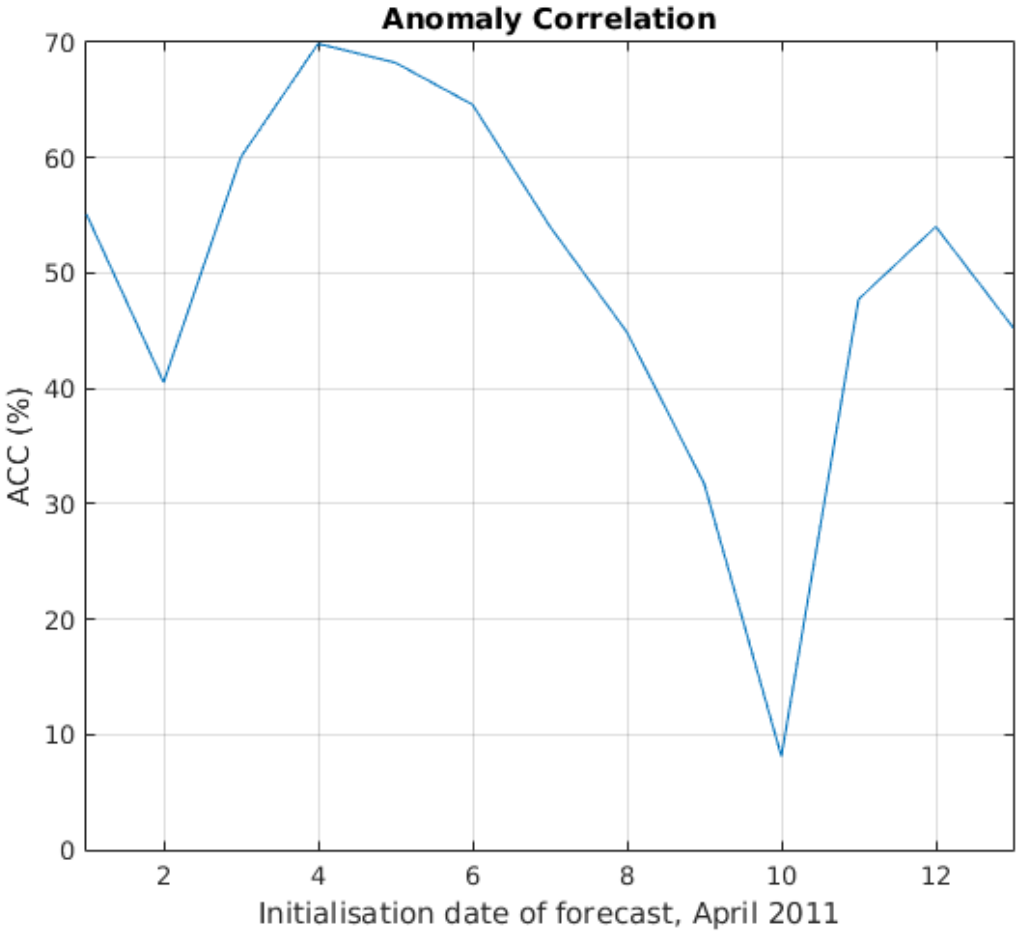

Figure 15. The anomaly correlation coefficient of 500 hPa geopotential height over Europe and the easternmost part of the North Atlantic on the 6th day of the 13 deterministic forecasts. The x-axis means the initialisation dates of the forecasts, and every forecast was initialised at 00 UTC. The deep dip on the 10th of April confirms that the bust occurs also in OpenIFS.

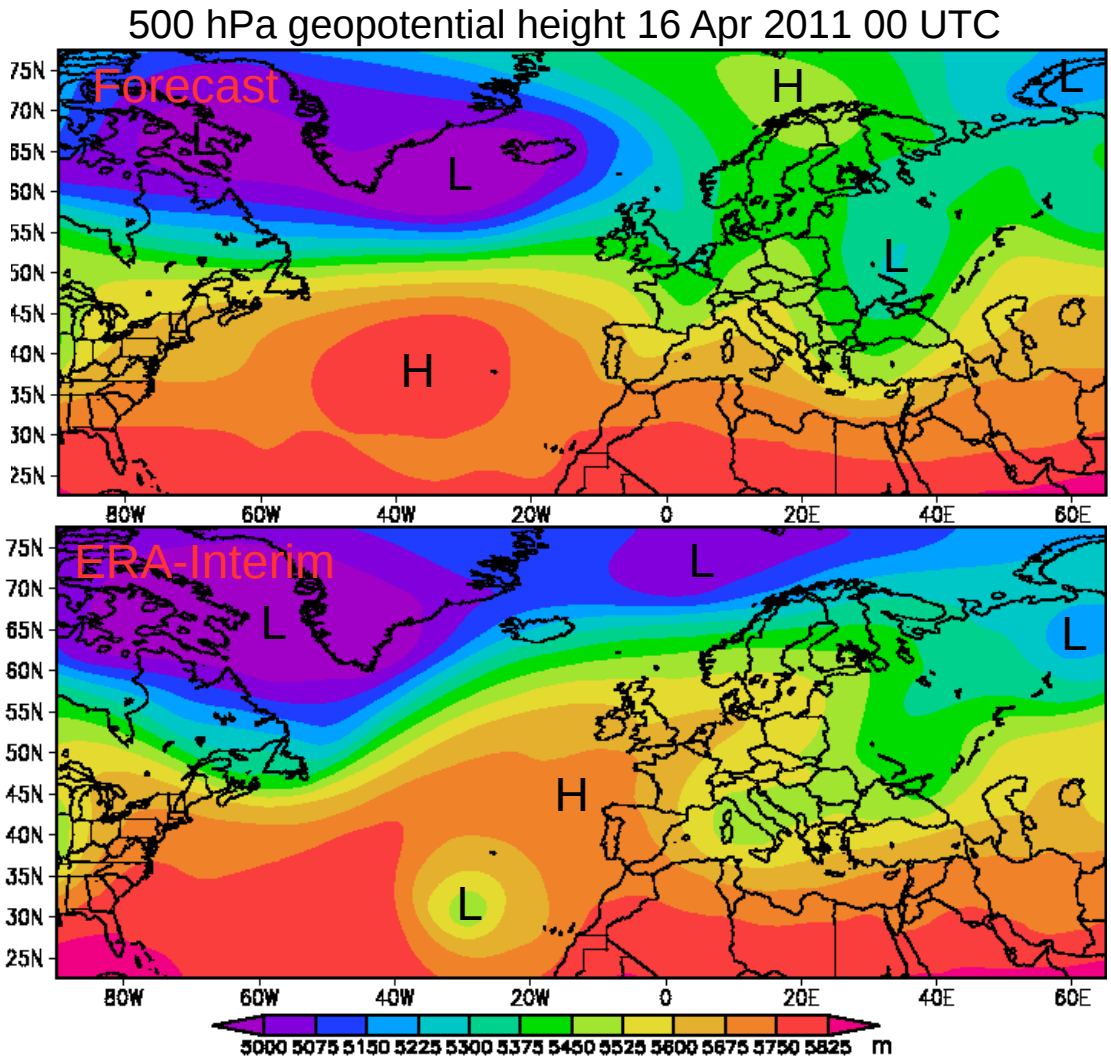

Figure 16. Day 6 forecast of 500 hPa geopotential height in the worst 6 day forecast (the control forecast) in terms of the ACC in figure 15 (the upper panel) and corresponding ERA-Interim reanalysis (the lower panel). The control forecast predicted formation of a blocking high over Northern Europe but according to the reanalysis the blocking never formed properly. The strongest negative contributions to the ACC in figure 15 come from the Northern Europe where there is the erroneous trough-blocking pattern and from the eastern North Atlantic where the control forecast missed the development of a cut-off low. The blocking stays over Northern Europe for the rest of the 10 day forecast.

As I had initial conditions only for 00 UTC for each day so I do not know whether OpenIFS would have produced a double bust if I had had initial conditions for other day times also. Actually the red curve depicting the performance of IFS in figure 5 and the curve depicting the performance of OpenIFS in figure 15 have pretty similar shapes when one excludes all other initialisation dates than those at 00 UTC

in figure 5. The performance of OpenIFS is generally lower than the performance of IFS because I used low resolution version of OpenIFS. Horizontal resolution of control forecast of IFS is T1279 which corresponds to about 16 km grid spacing. Instead horizontal resolution of T255 was used in my OpenIFS experiments. T255 corresponds to about 80 km grid spacing. One grid point is representing so large area that it can smooth out small scale features. This can have some effect in longer runs.

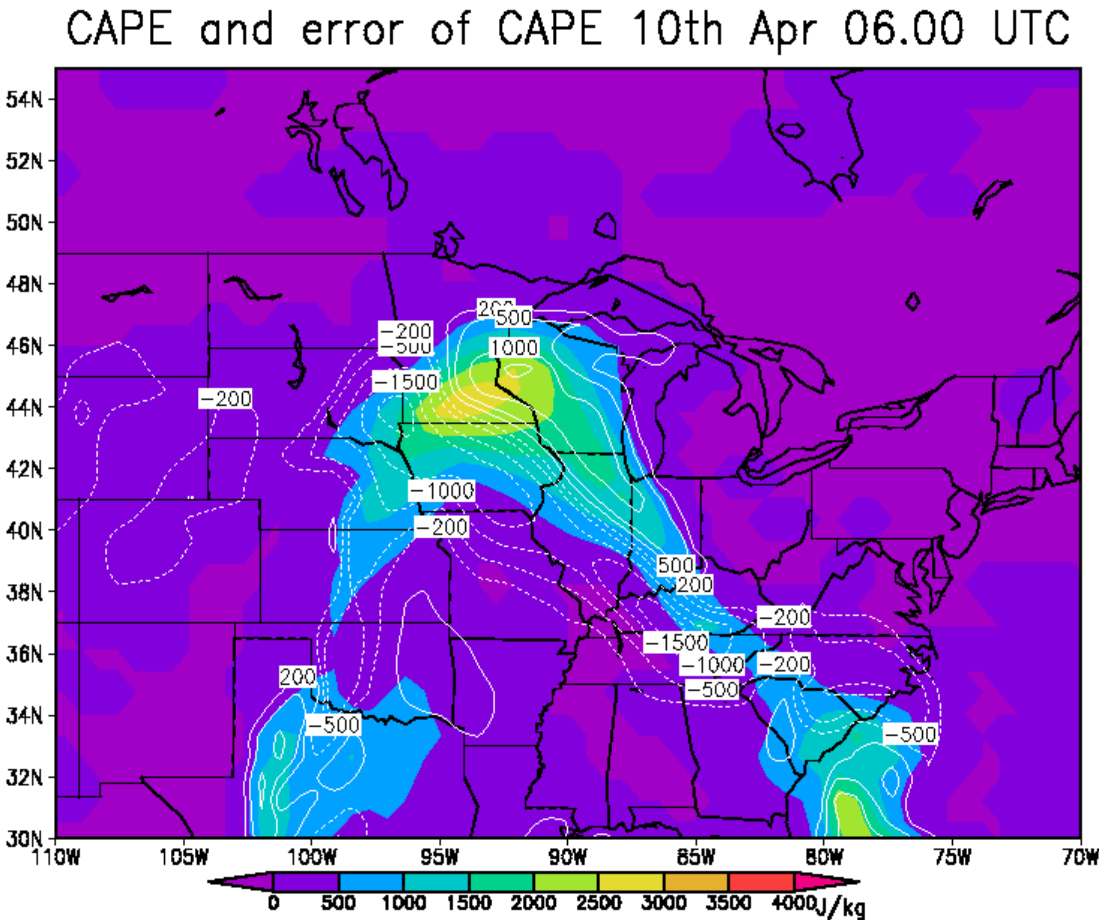

Figure 17. 6 hour forecast CAPE (shaded) in the control forecast and error of the CAPE (contoured, contour interval 500 J/kg). The error is the control forecast minus the reanalysis. The area of high CAPE is propagating too fast and too much eastward in the control forecast. The control forecast is also underestimating the CAPE. The error of CAPE will impact the mostly convective precipitation in the area later.

This forecast bust is quite extraordinary. Usually European forecast busts are related to situation where model could not forecast development of blocking. Instead in this case, OpenIFS entered into blocked regime but ERA-Interim reanalysis does not show signs of blocking on the 16th of April. Upper panel of figure 16 shows strong dipole pattern of a blocking high over Northern Europe and a deep trough

over Southern Greenland in the control forecast. ERA-Interim instead shows that the regime of westerly flow is prevailing. There is a trough on the place of the northern part of the blocking high north of Norway, and further south there are only signs of a weak mobile ridge. There is also a cut-off low instead of a ridge west of Canary Islands. The cut-off low is remnant of the third anticyclonic Rossby wave breaking during the six day period considered. This RWB is the one which is cyclonic in the control forecast but anticyclonic in the reanalysis but this will be discussed in more details later.

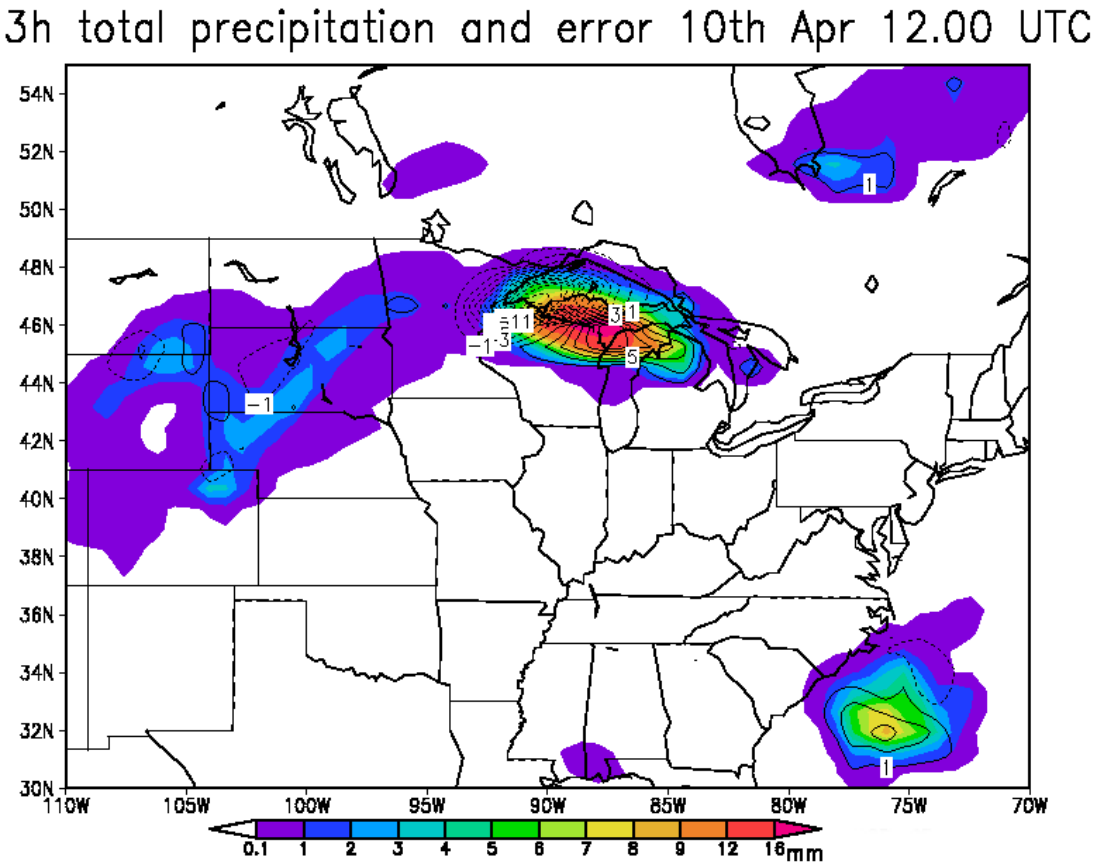

Figure 18. 3 h total precipitation (shaded) and error (contoured, contour interval 2 mm) 6 hours after figure 18. The error is the control forecast minus the reanalysis. The error in CAPE has caused the MCS west of the Great Lakes to move too fast eastward and to take too southerly track in the control forecast. Convection in wrong place causes upper tropospheric divergence in wrong place, and the erroneous divergence will cause errors in large scale dynamics which will eventually arrive in Europe.

As previous studies suggest that convection can cause forecast busts, I take a look at what happens over North America. First forecast of CAPE shows location and magnitude errors already in six hour forecast (figure 17). OpenIFS forecasts the area of CAPE too far north-east. OpenIFS also clearly underestimates the magnitude of CAPE. As CAPE tells how much energy the convection has available, the heaviest precipitation occurs often near the maximum of CAPE. Therefore error in CAPE field spreads to precipitation field (figure 18). The precipitation does not react instantaneously but it takes a couple of hours before the errors in CAPE field begin to affect the precipitation field. The area of high CAPE is moving pretty fast north-east in the control forecast while in reanalysis the area of high CAPE is moving almost straight northward and somewhat slower. At the beginning the precipitation related to the MCS west of the Great Lakes looks quite similar in the control forecast and the reanalysis but at the 9th hour of the forecast the differences begin to emerge. The error of CAPE field affects the precipitation so that the MCS is moving too fast north-east and on too southerly track on the 12th hour of the control forecast. The intensity of the MCS is roughly correct in the control forecast although there was a significant magnitude error in CAPE.

As there is precipitation in the wrong location, there must also be mid level ascent and upper level divergence in the wrong location. The effect of erroneous divergence can be studied using 300 hPa Rossby wave source fields and the fields have been calculated using equation [13]. One can make a general observation from figures 19 and 20 that the magnitude of the RWS is overestimated in the control forecast on the first three days of the forecast so that negative and positive values are both too large. As the values are overestimated in so large area, it looks like it is some artificial feature of OpenIFS or ERA-Interim. The method to calculate RWS was exactly the same for data from both OpenIFS and ERA-Interim. Also the input data for the calculation was exactly similar It is known that OpenIFS is not in balance at the beginning of the simulation, and therefore there are numerous small “disturbances” in figure 19 but it does not explain the overestimation in other figures. This feature makes it much more difficult to distinguish errors caused by the misrepresented convection. However, some real events can be seen. The areas of positive RWS initially generated by the convection (red ellipses in figure 19) are very pronounced through the 6 day forecast period.

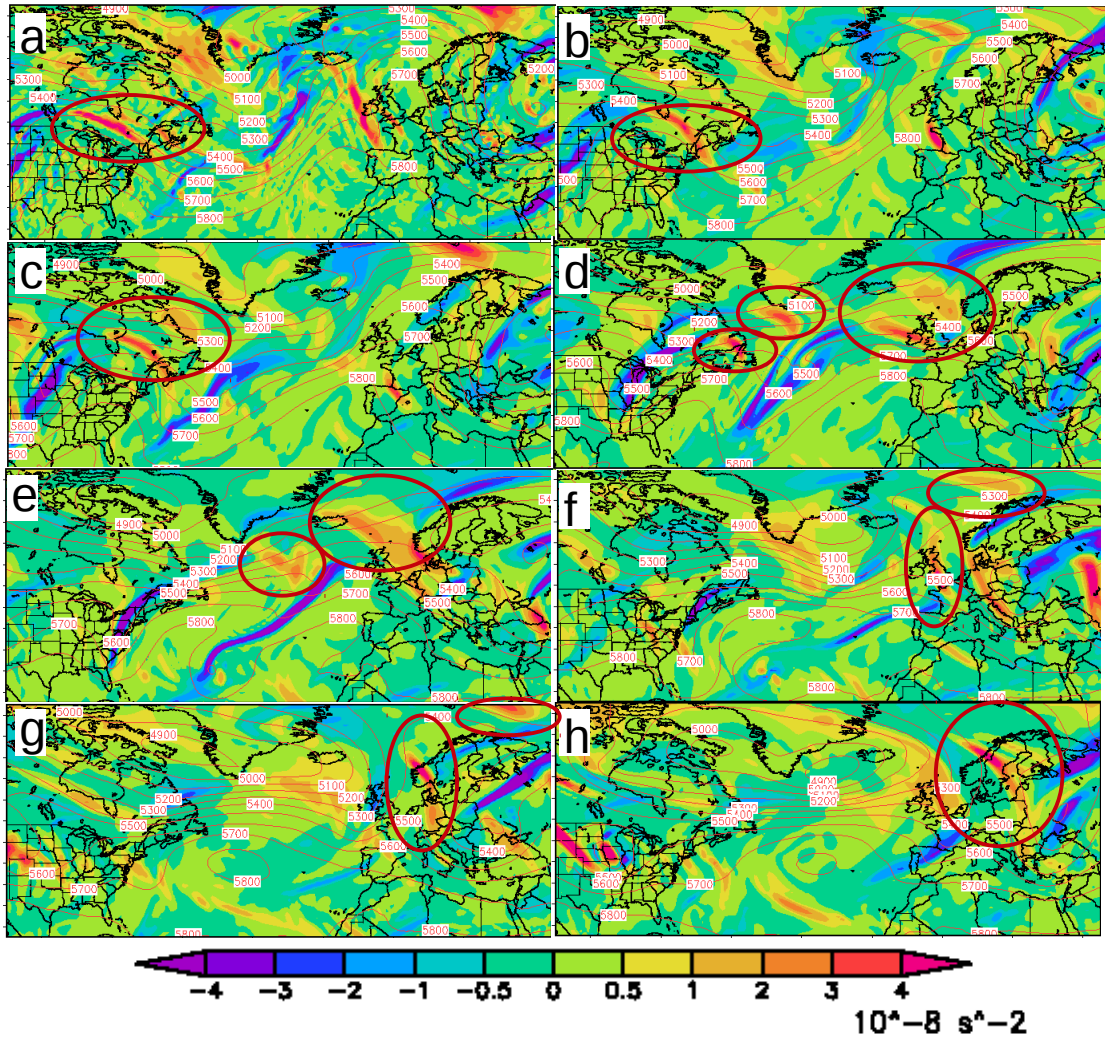

Figure 19. Rossby wave source on 300 hPa level (shaded) and 500 hPa geopotential height (contoured) in the control forecast. Areas of Rossby wave amplification generated by the North American convection are marked with ellipses. (a) 10 Apr 00 UTC, (b) 10 Apr 12 UTC, (c) 11 Apr 00 UTC, (d) 12 Apr 00 UTC, (e) 13 Apr 00 UTC, (f) 14 Apr 00 UTC, (g) 15 Apr 00 UTC and (h) 16 Apr 00 UTC. Where the values are positive, ridges are building up and where the values are negative, troughs become deeper so positive values at the top and negative values at the bottom of Rossby waves amplify them. The MCS creates strongly positive area of RWS which is moving east (panels a – c). As the energy of Rossby waves is moving at group velocity, another positive area of RWS forms over the Eastern Atlantic (panels d and e). The positive areas of RWS arrive over Europe, become very persistent and amplifies the ridge into blocking event (panels f – h).

Comparison of figures 19 and 20 show how especially the marked positive RWS areas are overestimated in the control forecast respect to reanalysis. This is seen in all panels a – h in figures 19 and 20. This is probably not only a feature of OpenIFS but

a real phenomenon caused by the misrepresented convection because the areas of positive RWS areas are so much weaker in the reanalysis (figure 20). The strong RWS in the control forecast seems to amplify the ridge forming over the Atlantic so much that it eventually forms blocking over Northern Europe. In the reanalysis instead, weaker RWS is only able to create a mobile ridge.

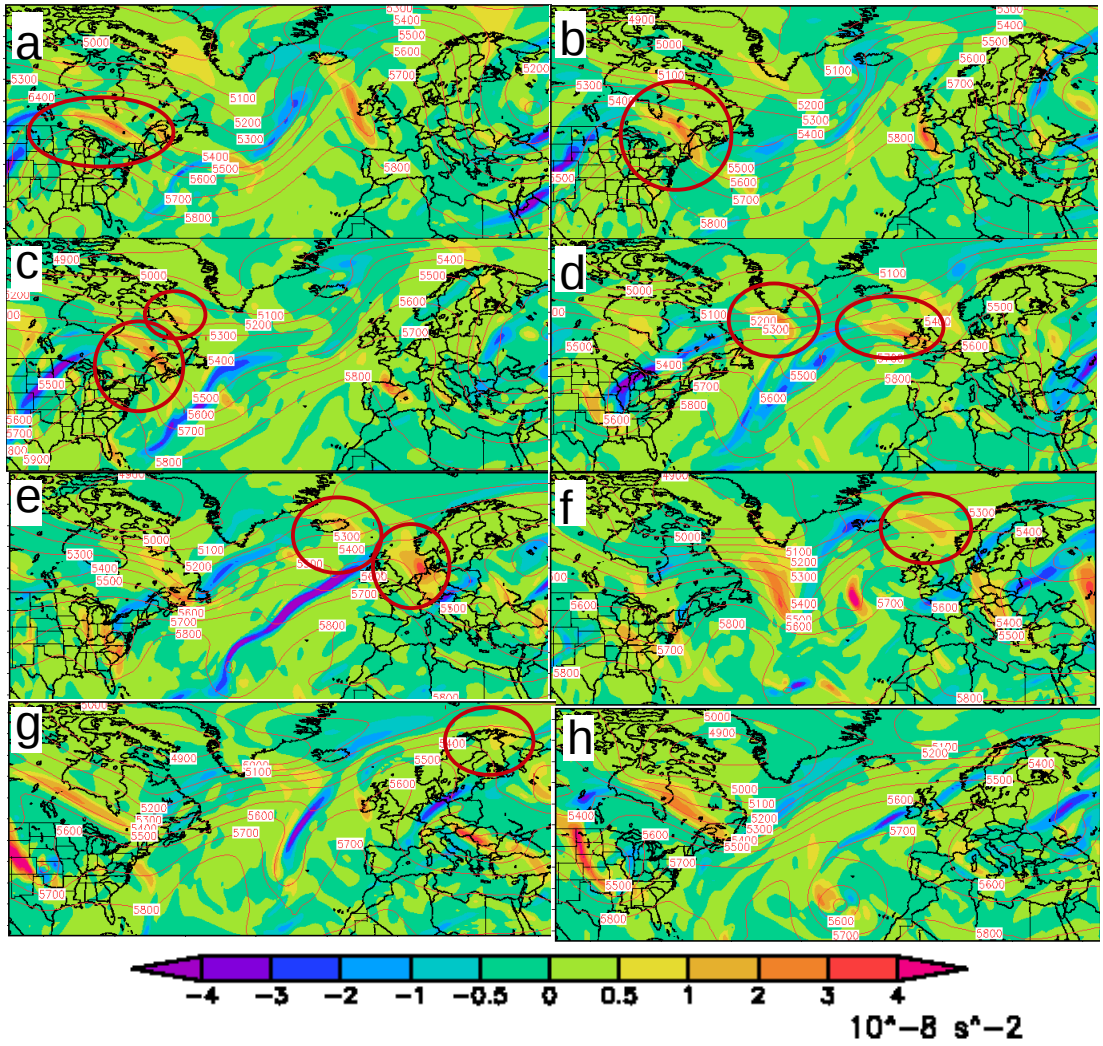

Figure 20. As in figure 19 but these are from ERA-Interim reanalysis. The areas of RWS are generally weaker than in figure 19. The evolution of RWS field is otherwise generally similar than in figure 19 but the positive areas do not stop over Europe in panels f – h but they continue to weaken and moving north-east. RWS is only able to create a mobile ridge over Europe.

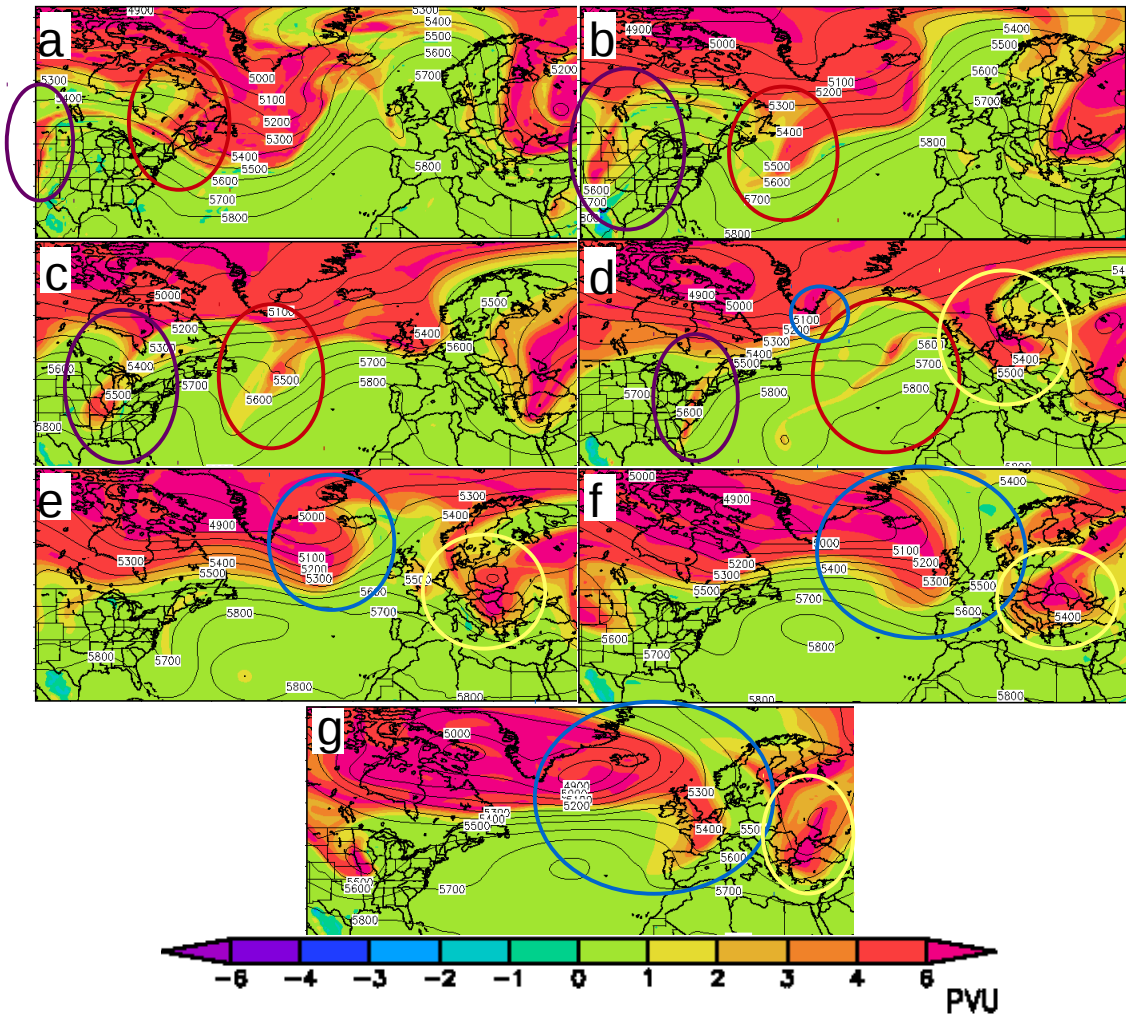

Figure 21. Potential vorticity on 315 K level (shaded) and 500 hPa geopotential height in the control forecast. (a) 10 Apr 00 UTC, (b) 11 Apr 00 UTC, (c) 12 Apr 00 UTC, (d) 13 Apr 00 UTC, (e) 14 Apr 00 UTC, (f) 15 Apr 00 UTC and (g) 16 Apr 00 UTC. Coloured ellipses denote individual Rossby waves associated with RWB activity occurring after North American convection. The troughs immediately east and west of North American convection (red and purple ellipses in panels a – d) break anticyclonically. There is also a cyclonic RWB over Europe (yellow ellipses in panels d – g) that might feel the effect of errors because of downstream development of Rossby waves. The trough denoted with purple ellipses redevelops and breaks cyclonically (blue ellipses in panels d – g). The trough in purple and blue ellipses is the same trough as the Rockies´ trough in figure 13.

Because it is known that blocking is associated with Rossby wave breaking, I looked at potential vorticity on 315 K level. PV is the best indicator of RWB as it shows the air masses that are cut off the main air mass. In the figures 21 and 22 one can see that the Rossby wave train, which originates from North America, breaks only two times anticyclonically in the control forecast whereas in the reanalysis the

wave train breaks three times anticyclonically over the Atlantic and Europe. All RWB events occurring in the area of interest are identified with coloured ellipses in figures 21 and 22. The first two anticyclonic RWBs (figures 21 and 22, panels a – d, pink and red ellipses) and the first cyclonic RWB (figures 21 and 22, panels d – g, yellow ellipses) occur almost identically in the control forecast and the reanalysis. It is, though, probable that the cyclonic RWB denoted with yellow ellipses, is not affected by the errors of North American convection.

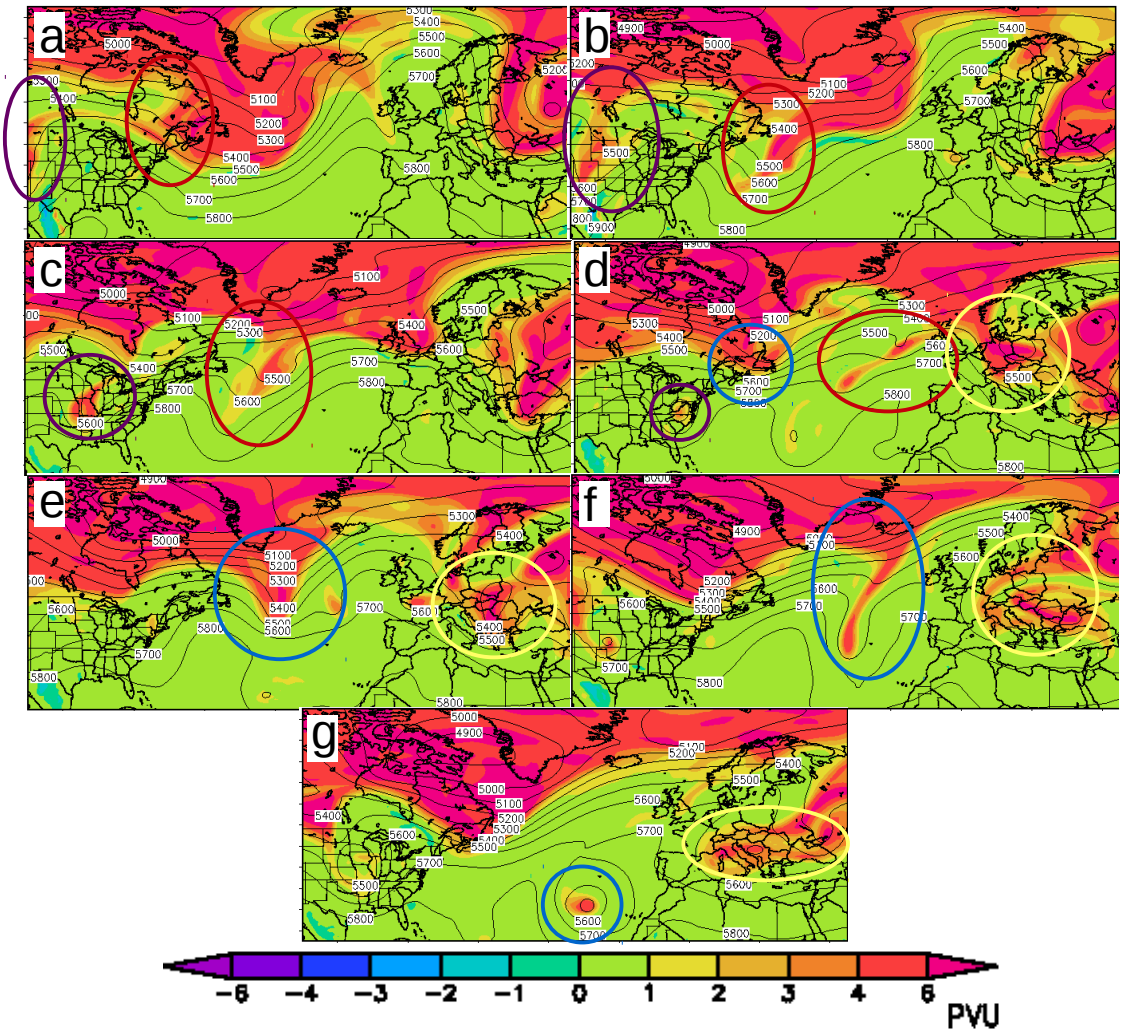

Figure 22. As in figure 21 but from ERA-Interim reanalysis. The first three RWBs (red, purple and yellow ellipses in panels a – g) occur similarly as in the control forecast in figure 21. However, the ex Rockies´ trough (blue ellipses in panels d – g) breaks anticyclonically, not cyclonically as in figure 21. After this anticyclonic RWB westerly flow prevails over Northern Europe and the blocking event is cancelled.

The RWB event identified with blue ellipses (figures 21 and 22) occurs cyclonically in the control forecast and anticyclonically in the reanalysis. The Rossby

wave associated with this RWB is the same wave as the one with the Rockies´ trough in figure 12 in chapter 4.1. In the control forecast this wave does not evolve over the Atlantic in such a way that it could break anticyclonically whereas in the reanalysis the wave evolves, amplifies and breaks anticyclonically like a text book example. It looks like the RWB in the reanalysis identified with blue ellipses cancelled already ongoing formation of a blocking high. The misrepresented convection seems to have caused a small error to the Rockies´ trough which grows and spreads gradually and becomes finally clearly visible on the third day of the control forecast.

4.3. Ensemble forecast

I have ensemble initial conditions for 50 members but I chose the five first members for the worst day to start a 6 day forecast. I wanted to generate different outcomes and see if some of the members performed better than others and at the same time keep this experiment compact. None of the chosen members performed well. Figure 23 shows that I got variance in terms of the day 6 ACC of 500 hPa geopotential height over Europe. Two members performed slightly better and three worse than the control forecast. Actually the fifth member performed the best and the second performed the worst in terms of the ACC over Europe. Figure 24 shows a spaghetti plot of 5400 metre contour of 500 hPa geopotential height. All of the ensemble members predicted blocking over Europe on the 6^{th} day of forecast although there are large differences in shape, strength and exact location of the blocking among the ensemble members. However, every ensemble member is pretty far from the reanalysis representing the truth (black contour in figure 24) and actually the ensemble mean is quite similar to the control forecast (figure 25). The blocking only occurs a few hundred kilometres further east in the ensemble mean. On the other hand the flow is very zonal over the Atlantic in all forecasts whereas the reanalysis shows tilted flow. OpenIFS seemed not to be extremely sensitive to the perturbations in the five first members as all forecasts ended up in the same blocked regime. However at least in IFS there is also such a member that clearly ends up in the right regime of westerly flow as the ACC is high as can be seen in figure 4 in chapter 2.1. but I did not happen to choose that member. The results of this chapter are highly dependent of my chosen ensemble members. The results may have differed considerably if I had chosen either 5 different members or more members.

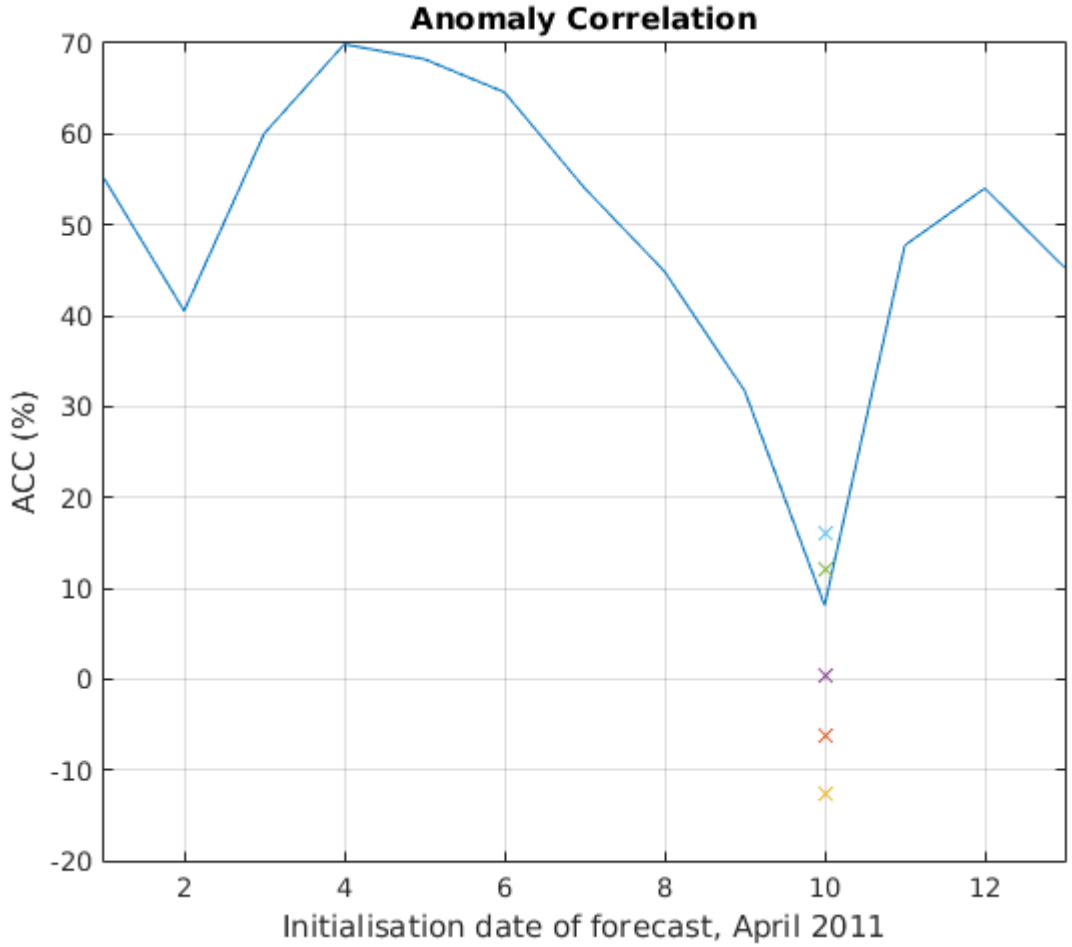

Figure 23. As in figure 15 but now there are also the ACCs of the five ensemble members marked with crosses of different colours on the 10th of April. The ensemble forecast provided some variation but less than expected. Mean of my ensemble forecast is less skilled than the control forecast. This means that the ensemble forecast was a bad one.

All ensemble members are different because the initial conditions are different. In 500 hPa geopotential height and mean sea level pressure fields the initial perturbations concentrate on the trough-ridge system over North America. The perturbations are there where I assumed the bust to originate. This means that the algorithm that has created the initial conditions has recognised the area of potential errors. Let us consider especially the initial conditions of members 5 (figure 26 a) and 2 (figure 26 b) which are the best and the worst members of my ensemble forecast in terms of the ACC. In 500 hPa geopotential height initial conditions the recipe for better performance over Europe is making the trough over the Rockies 10 – 15 m deeper, and increasing the gradient between the trough and the ridge over Mid West of the US and not making significant changes to other parts of the ridge.

Instead decreasing the geopotential height at the top of the ridge made the outcome worse. In sea level pressure initial conditions, making the low pressure weaker, improved the outcome (figure 27 a). On the other hand making the surface low deeper caused the outcome to become worse than in the control forecast (figure 27 b).

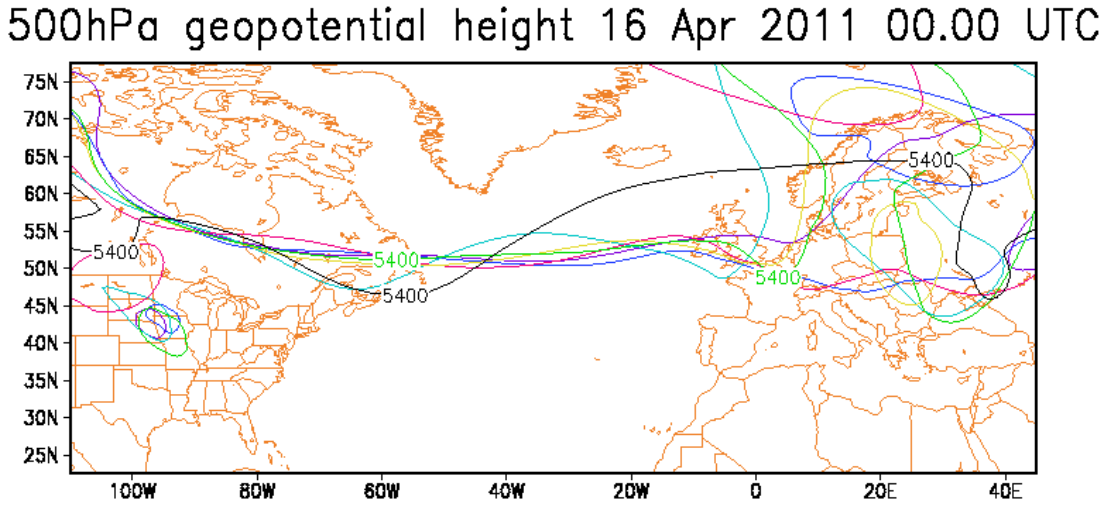

Figure 24. A spaghetti plot of 5400 metre contour of 500 hPa geopotential height on the 6th day of the ensemble forecast. Green contour is the control forecast, black contour is the reanalysis which represents the truth and other contours are the five ensemble members. Figure shows how there is variation among individual forecasts over Europe and less variation to west of Europe showing how the area of poor predictability has formed over Europe. Despite the variation, the forecasts were quite consistent that some kind of blocking high will form over Europe. There is no sign of blocking in the reanalysis but westerly flow prevails.

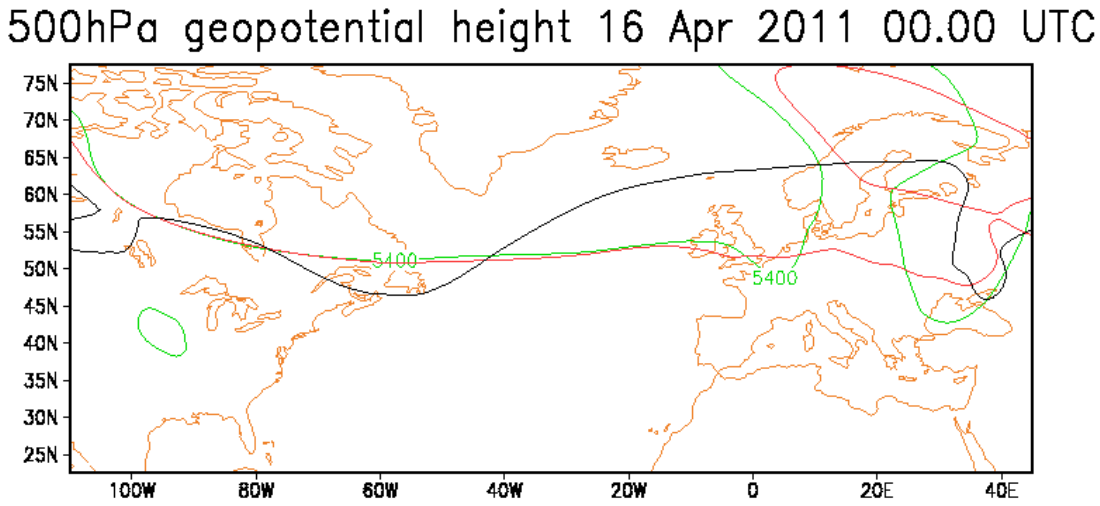

Figure 25. As in figure 24 but in this figure the red contour represents the ensemble mean. The ensemble mean is not better than the control forecast. The blocking high is only forecast to locate slightly further east than in the control forecast.

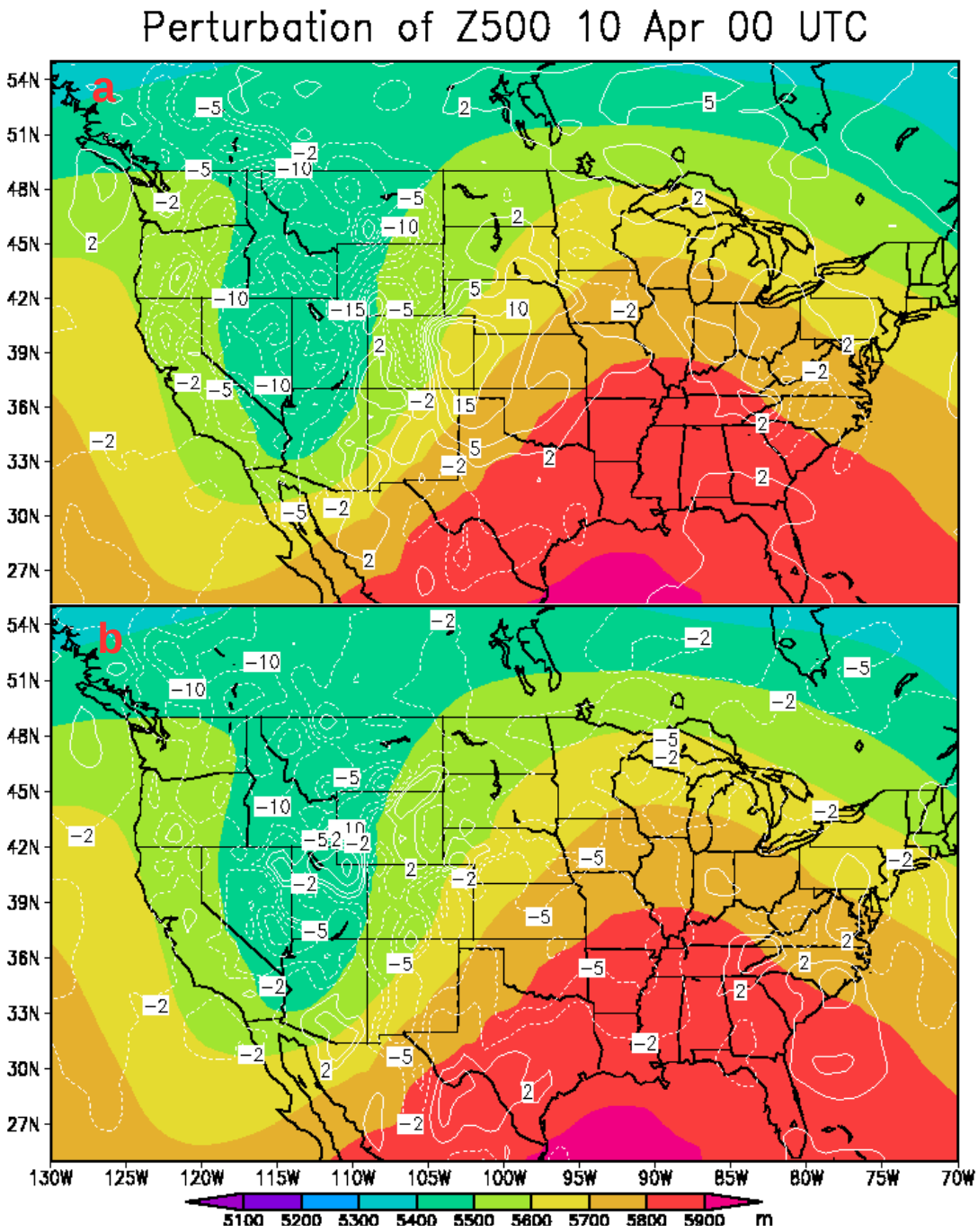

Figure 26. Initial perturbations of 500 hPa geopotential height. Panel (a) is the 5th ensemble member that is the best and panel (b) is the 2nd ensemble member that is the worst. 500 hPa geopotential height of the control forecast is shaded and initial perturbations of the ensemble members are contoured. Panel (a) shows that the trough-ridge pattern is amplified in the best member. Especially the height gradient is larger in the Central US. Panel (b) shows that there is large negative perturbation both in the trough and the ridge so the pattern is less amplified compared to panel (a).

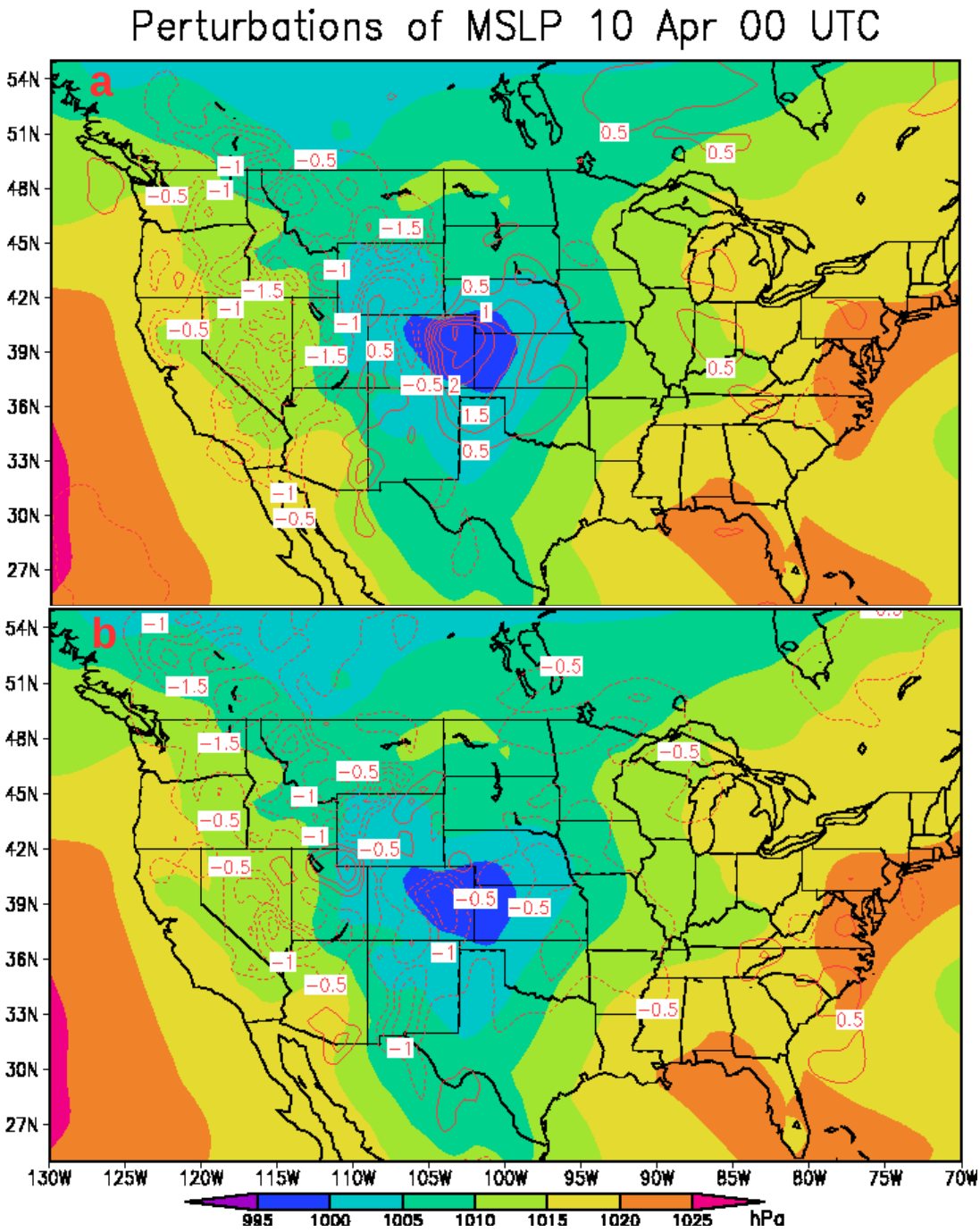

Figure 27. Initial perturbations of sea level pressure. Sea level pressure of the control forecast is shaded and sea level pressure perturbations are contoured (unit hPa). Panel (a) shows perturbations in the best member. There is a positive perturbation of 2.5 – 3.0 hPa in the developing surface low. The low is considerably weaker than in the control forecast. Panel (b) shows perturbations in the worst member. There is negative perturbation of 0.5 – 1.5 hPa in the surface low so it is stronger than in the control forecast.

Evolution of CAPE in short forecasts over North America are rather surprising compared to the outcomes over Europe (not shown). I expected the CAPE to behave more like in the reanalysis in the most skilled ensemble members as the best member has 30 % units better ACC than in the worst one but this is not the case. First of all, the differences between the ensemble members are almost an order of magnitude smaller than the differences between the control forecast and the reanalysis. Second, the area of maximum CAPE is even further east in the best ensemble member compared to the control forecast. I expected it to be the opposite as the maximum of CAPE was further west in the reanalysis. However, one must remember that my ensemble was not particularly skillful so a pattern which improves the forecast considerably was not found although some signs show that the Rockies´ trough should be more amplified than it is in the control forecast. This result is actually in agreement with results found by Rodwell et al. (2013). They also found that deeper trough leads to better performance.

5. Discussion

5.1. Development of the forecast bust

The purpose of this study was to determine if the incorrect representation of convection over North America lead to a forecast bust over Europe. Besides this main goal, this study also identifies the chain of events leading to the forecast bust and finds some patterns from the initial conditions causing the bust. Now I reflect my results to a more general study of Rodwell et al. (2013). According to Rodwell et al. (2013) my forecast bust is very typical spring time bust case. The characteristic Rockies´ trough was present in this case and there was a ridge east of it. This is the first link of the chain. Another striking similarity with a typical spring bust was the area of high CAPE. Also the presence of a surface low east of the trough caused wind shear which partly overlapped the area of high CAPE. This made the atmospheric conditions favourable for strong convection. This is the second link. A MCS initiated in the area of high CAPE a couple of hours before the initialisation of the forecasts.

The impact or effect of the errors in the initial conditions and possibly also of the model parametrisations became visible already in the 6 hour forecast of CAPE. The

control forecast predicted too little CAPE and too far east. This is the third link. As a side remark, the error in CAPE tells that there have to be significant errors in other fields also, at least in temperature and moisture fields because CAPE is a function of temperature and moisture. These errors were not considered in details in this study as I concentrated on the convection. Anyway, the erroneous CAPE field had a strong influence on the precipitation. Already in the 9 hour forecast the MCS south-west of the Great Lakes has began to veer too much east towards the maximum in the erroneous CAPE field. This is the fourth link in the chain. Later on the location error of the MCS keeps on growing.

The misrepresented MCS existed for about 15 hours so it had plenty of time to cause upper level divergence in wrong place. Divergence is the link to the large scale dynamics (not shown). Upper level divergence causes upper level divergent wind. The Rossby wave source, which acts to amplify Rossby waves, is the gradient of divergent wind multiplied by absolute vorticity. Therefore, strong convection tends to cause RWS. The error in RWS seems to be quite small in the Great Lakes´ area though. One suggestion for the absence of clearly visible error could be that an isolated MCS cannot produce strong and widespread divergent wind after all. Another reason for this could be that the coarse resolution of OpenIFS obscured some small scale features. Spherical truncation of T255 equals to 78 km grid spacing so the MCS fits well in a 10 by 10 grid points area. However, from the theory of RWS in section 2.4 I can conclude that misrepresented convection must cause misrepresented RWS although the effect is most clearly visible several hundred kilometres north-east of the convection. The over and underestimation of RWS values in the control forecast may be some artificial bias of output of OpenIFS or ERA-Interim and it would not have further implications but it is also possible that there is something in the parametrisations. This was not investigated further in this study. Overall, the erroneous RWS is the fifth link of the chain.

For a couple of days the error in the Rossby wave remains small. On the 3rd and 4th days of the control forecast the error growth accelerates and begins to affect how the Rossby wave breaks over the Atlantic. In the control forecast one wave breaking occurs in more cyclonic way whereas in ERA-Interim reanalysis the same wave breaking is clearly anticyclonic. The misrepresented wave breaking is the sixth link of the chain. This is the bifurcation point where the error that had remained relatively small suddenly grows into large proportions and the forecast and the truth lose

correlation. Interestingly this rapid growth of error is confined over North Atlantic and Europe but it is reasonable if one thinks about downstream development and group velocity of Rossby waves. The area of error propagated roughly at group velocity. This wave breaking process seems to have been the event which was exceptionally sensitive to the initial errors originating from the Rocky Mountains. The final seventh link of the chain is how the modelled cyclonic RWB created a large area of low PV over Northern Europe that resulted in development of a blocking event whereas in the reanalysis the anticyclonic wave breaking prevented the formation of large isolated area of low PV so the westerly flow prevailed.

5.2. The ensemble forecast

The ensemble forecast of five members that I ran for the same day as the control forecast proved not to be a great success although I was able to extract some information from the experiment. Every member ended up in almost similar state as the control forecast and the skill of the ensemble mean was actually worse than of the control forecast. Now, looking back, I should not have chosen the first five members of 50 but choose five random members. The problem of our systematically chosen ensemble was that the perturbations in the initial conditions were not diverse enough as odd ensemble members have positive perturbation and even members have negative of the same perturbation. If I had had been accurate enough when conducting this experiment, I could have utilized the hint provided by Rodwell et al. (2013) that strengthening the trough-ridge pattern over the Rockies in the initial conditions improves the skill of day 6 forecast over Europe. Although our ensemble forecast did not perform well, I got results which agree with that result in Rodwell et al. (2013). Also I discovered that making the Rockies´ trough deeper and the ridge higher improves the result over Europe. On the other hand Rodwell et al. (2013) say that it is also possible that the amplified wave pattern over North America might precorrect error caused by other unknown error or model parametrisations so I cannot say for absolutely sure that the bust was caused solely by errors in initial conditions although I consider the initial conditions to be the most likely source of errors.

So am I content on how we treated the research question in this study? Yes and no. The study of the control forecast was quite comprehensive. I was able to find

evidence that the misrepresented North American convection has indeed something to do with European forecast bust 6 days later. I was also able to show the full chain of events leading to the forecast bust over Europe all the way from the US. I managed to reproduce many of the results shown by Rodwell et al. (2013) and partly I went even deeper in details. Instead I cannot be entirely happy with my ensemble forecast experiment although it provided some information.

5.3. Making forecasts more reliable

Based on this study one might ask that are these weather situations involving Rockies ´ trough hopeless initial conditions for weather forecast? First, trough over the Rocky Mountains is rather common but not every case involving the trough leads to forecast bust. Figure 6 in chapter 2.1. shows that forecast busts occur only a couple of times per year. However everyone who reads this study will be aware that a forecast bust can occur when there is a trough over the Rockies and large CAPE over the Mid-West of the US. Already knowing this possibility adds a bit value in forecasting. In ensemble forecasting there is also one red flag telling when a forecast bust may occur. Rodwell et al. (2013) tell that spread of ensemble forecast systematically increases a few days ahead of onset of European blocking so one can think the increase in spread as a qualitative measure of likelyhood that the forecast will fail.

Numerical improvement of forecasts can be done in initial conditions, in model parametrisations and by increasing number of grid points. All of these are actually being worked on but progression is not fast because it is limited by computational resources. Assimilating more accurate initial conditions is extermely computationally demanding. Increasing number of gridpoints improves forecasts to some extent as less parametrisation is needed. Thus, computational expences grow rapidly because of smaller grid point spacing increases number of calculations. Improving parametrisations is not easy as many phenomena are not well known and many phenomena are difficult to quantify. This is the main problem of the parametrisations. It is often difficult to describe subgrid scale phenomena so that the parametrisation works well, is physically reasonable and is computationally cheap. However every new version of a NWP model usually contains something new so it would be interesting to see would newer cycle of OpenIFS CY40r1 perform better than the older version CY38r1 used in this study. Despite all of the improvements, We may

never get completely rid of forecast busts because we may never be able to solve all microphysical processes explicitly in NWP models so parametrisations will be needed also in the future and we may never be able to create perfect initial conditions. However, probably the easiest and fastest way to increase reliability of forecasts is to increase number of high quality observations in areas where the busts most often originate from.

5.4. Possible further directions

Here I propose a couple of ideas how this forecast bust could be studied further. OpenIFS can be run with or without stochastic physics and the switch is also easy to use. This spawns two new research topics. Both would try to give an answer to question that do the model parametrisations have effect on skill scores over Europe in this bust case and is it possible quantify this improvement. Both experiments would utilize stochastic physics of the SPPT scheme (Palmer et al. 2009) in OpenIFS. One experiment would be to compare an ensemble forecast with ensemble initial conditions and stochastic physics to an ensemble forecast with the same initial conditions but without stochastic physics. Another experiment would be to compare an ensemble forecast created with stochastic physics using only one set of initial conditions to a regular ensemble forecast with only ensemble initial conditions. This bust is probably mostly caused by errors in the initial conditions but because strong convection is included, I cannot state that the model parametrisations do not play a role. In all modern NWP models convection is highly parametrised phenomenon so something could be found there.

At early steps of this study I considered to study correlation between skill score of precipitation and CAPE over the US, and the ACC of 500 hPa geopotential height over Europe 6 days later. Calculation of skill score for discontinuous fields like precipitation and CAPE is difficult because the double counting of errors needs to be avoided. Thus, Wernli et al. (2008) have designed an algorithm for calculating skill score for discontinuous fields. This algorithm is complicated and challenging to code so that is why I did not conduct this study. The hypothesis that some correlation could be found was also critisized to be naïve but on the other hand I have not come across a paper where this hypothesis is proved right or wrong.

The third suggestion requires manual manipulation of the initial conditions. As

misrepresented precipitation is one key component of the bust, maybe the skill of day 6 forecast over Europe could be improved by doing manual modifications to precipitation over the US. This could be done for example by modifying moisture observations and generating new initial conditions by data assimilation. For example either one or both of the two MCSs could be weakened or even removed by decreasing the mixing ratio. The point of this experiment would be to confirm that misrepresented convection is not only a symptom of developing bust but plays an active role as is suggested by Rodwell et al. (2013). They have looked at diabatic PV tendency caused by convection. Removal of parts of convection would be a step more radical way to inspect the interaction between the convection and the Rockies´ trough. One has to remember also that in this experiment there is risk of precorrection of error so that results could improve because of errors cancelling each other. The modification of initial conditions so that the model does not crash or produce totally unreasonable result may be challenging too.

6. Summary and conclusions

April 2011 forecast bust was a typical spring bust case (Rodwell et al. 2013, Grazzini and Isaksen 2002). A trough located over the Rockies and was moving towards east. A surface low developed east of the upper level trough in the area of forcing provided by the trough. This surface low induced southerly flow of warm and moist air from Gulf of Mexico to Mid-West of the United States. In the Mid-West the warm and moist surface air mass went under cooler mid and upper level air mass which lead to build-up of CAPE in a deep layer. Moreover the strong warm advection in the Mid-West caused substantial wind shear which helps individual thunderstorm cells to cluster into a mesoscale feature. The ERA-Interim reanalysis showed that the atmospheric condition was very favourable for strong convective event just before the initialisation of the control forecast. Strong convection is already recognised to be one source of European busts (Rodwell et al. 2013, Grazzini and Isaksen 2002).

Two separate MCSs were found at the beginning of the control forecast on the 10th of April. The stronger one located southwest of the Great Lakes over Nebraska area. This MCS was moving towards the Great Lakes. The weaker one located over the Eastern US in North and South Carolina. This MCS was moving towards the Atlantic. Because Rodwell et al. (2013) stated that the European forecast busts are

often caused by strong convection over the Great Lakes´ area I concentrated on the MCS in the Mid-West.

I had a suggestion that the strong convection could effect the large scale dynamics and eventually the effect would be felt in Europe because of this. I began the investigation of the control forecast with CAPE field on the 10th of April and found significant displacement and magnitude errors. This error lead to displacement error of the MCS in the Great Lakes´ area. When precipitation occurs in a wrong place there is also upper level divergence in wrong place. This can be seen in the Rossby wave source fields over eastern North America. Especially positive values in Eastern Canada are overestimated so the Rossby wave amplified too much in the control forecast. For a couple of days the error in the dynamics remained small but became evident on the fourth and fifth day of the forecast when the forecast predicted cyclonic RWB whereas in the reanalysis the same Rossby wave broke clearly anticyclonically. The cyclonic RWB in the control forecast created the blocking high over Northern Europe but in the reanalysis the anticyclonic RWB prevented the formation of large area of low PV so westerly wind prevailed.

As the last part of this study I selected five first members of a 50 member ensemble of ECMWF. The ensemble forecast of five members generated some spread but even the best member was only slightly better than the control forecast so the ensemble forecast was not particularly good one. Every ensemble member as well as the control forecast predicted formation of a blocking high over Northern Europe whereas the reanalysis did not show signs of blocking. Moreover, skill of the ensemble mean was worse than of the control forecast. However, as there were differences in the skill of the individual ensemble members, I studied the initial conditions also. I found that amplification of the Rockies´ trough-ridge pattern in the initial conditions improves the day 6 ACC over Europe. But as the improvement caused by amplification of the trough by 10 – 15 m respect to the control forecast corresponded to improvement of about 10 % units of ACC, I cannot say for sure that this is the best way to improve the initial conditions. Anyway also Rodwell et al. (2013) support the idea that the forecast bust has something to do with the trough.

All in all OpenIFS seemed to be exceptionally sensitive to some certain type of error in initial conditions. There are always errors in initial conditions but in this case the error happened to be located in an area that was very favourable for growth of errors. In this study I could not pinpoint where the error exactly is but this study

showed signs that the error has something to do with the Rockies´ trough and convection over Mid-West.

References

Ahlquist, J.E., (1985). Climatology of Normal Mode Rossby Waves, *Journal of the Atmospheric Sciences*, 42(19), pp. 2059 – 2068. Available at: http://dx.doi.org/10.1175/1520-0469(1985)042<2059:CONMRW>2.0.CO;2

Dee, D.P. et al., 2011. The ERA-Interim reanalysis: configuration and performance of the data assimilation system. *Quarterly Journal of the Royal Meteorological Society*, 137(656), pp.553–597. Available at: http://dx.doi.org/10.1002/qj.828.

Grazzini, F., & Isaksen L., 2002: North American increments. ECMWF OD/RD Memo.

GFS Analysis 2014. http://www.met.nps.edu/~hmarcham/2014.html

Hitchman, M.H. & Huesmann, A.S., 2007. A Seasonal Climatology of Rossby Wave Breaking in the 320–2000-K Layer. *Journal of the Atmospheric Sciences*, 64(6), pp.1922–1940. Available at: http://dx.doi.org/10.1175/JAS3927.1.

Holton, J. & Hakim G., 2013: An Introduction to Dynamic Meteorology, Elsevier, Waltham, Massachusetts, US, pp. 112, 160, 162.

Inness P. & Dorling S., (2013). Operational Weather Forecasting, John Wiley & Sons, Ltd, The Atrium, Southern Gate, Chichester, West Sussex, UK, 210.

James, I., 1994: Introduction to Circulating Atmospheres, Cambridge University Press, Cambridge, UK, pp. 263 – 270.

Kalnay, E., (2011). “Fighting chaos” in weather and climate prediction, Presentation in WMO meeting. https://www.atmos.umd.edu/~ekalnay/pubs/Chaos-Predictability-EnKF-WMOtalk.pdf

Lackmann, G., (2011). Midlatitude Synoptic Meteorology, American Meteorological Society, Beacon Street, Boston, Massachusetts, US, pp. 51, 85, 89, 294 – 295.

Lorenz, E.N., (1963). Deterministic Nonperiodic Flow, *Journal of the Atmospheric Sciences*, 20(2), pp. 130 – 141. Available at: http://dx.doi.org/10.1175/1520-0469(1963)020<0130:DNF>2.0.CO;2

Masato, G., Hoskins, B.J. & Woollings, T.J., 2012. Wave-breaking characteristics of midlatitude blocking. *Quarterly Journal of the Royal Meteorological Society*, 138(666), pp.1285–1296. Available at: http://dx.doi.org/10.1002/qj.990.

Ollinaho, P. et al., 2013. NWP model forecast skill optimization via closure parameter variations. *Quarterly Journal of the Royal Meteorological Society*, 139(675), pp.1520–1532. Available at: http://dx.doi.org/10.1002/qj.2044.

OpenIFS webpages https://software.ecmwf.int/wiki/display/OIFS/About+OpenIFS

Palmer, T.N. et al., 2009. Stochastic parametrization and model uncertainty. *Technical Memorandum*, (598).

Postel, G.A. & Hitchman, M.H., (1999). A Climatology of Rossby Wave Breaking along the Subtropical Tropopause, *Journal of the Atmospheric Sciences*, 56(3), pp. 359 – 373. Available at: http://dx.doi.org/10.1175/1520-0469(1999)056<0359:ACORWB>2.0.CO;2

Pu, Z.-X. et al., 1997. Using forecast sensitivity patterns to improve future forecast skill. *Quarterly Journal of the Royal Meteorological Society*, 123(540), pp.1035–1053. Available at: http://dx.doi.org/10.1002/qj.49712354012.

Reinhold, B., 1987. Weather Regimes: The Challenge in Extended-Range Forecasting. *Science*, 235(4787), pp.437–441. Available at: http://science.sciencemag.org/content/235/4787/437.

Rodwell, M.J. et al., 2013. Characteristics of Occasional Poor Medium-Range Weather Forecasts for Europe. *Bulletin of the American Meteorological Society*, 94(9), pp.1393–1405. Available at: http://dx.doi.org/10.1175/BAMS-D-12-00099.1.

Ruosteenoja, K. & J. Räisänen, 2013: Ilmakehän virtausrakenteiden dynamiikan lisämoniste. Department of Physics in University of Helsinki, pp. 21

Schultz, D.M., Keyser, D. & Bosart, L.F., (1998). The Effect of Large-Scale Flow on Low-Level Frontal Structure and Evolution in Midlatitude Cyclones, *Monthly Weather Review*, 126(7), pp. 1767 – 1791. Available at: http://dx.doi.org/10.1175/1520-0493(1998)126<1767:TEOLSF>2.0.CO;2

Thorncroft, C.D., Hoskins, B.J. & McIntyre, M.F., 1993. 2 Paradigms of Baroclinic-

Wave Life-Cycle Behaviour. *Quarterly Journal of the Royal Meteorological Society*, 119(509, A), pp.17–55.

Tibaldi, S. & Molteni, F., 1990. On the operational predictability of blocking. *Tellus A*, 42(3), pp.343–365. Available at: http://dx.doi.org/10.1034/j.1600-0870.1990.t01-2-00003.x.

Wernli, H. et al., 2008. SAL—A Novel Quality Measure for the Verification of Quantitative Precipitation Forecasts. *Monthly Weather Review*, 136(11), pp.4470–4487. Available at: https://doi.org/10.1175/2008MWR2415.1.